Antiferromagnetism and Superconductivity

Boulder School for Condensed Matter and Materials Physics
July 14, 15, 2014
Subir Sachdev

Talk online: sachdev.physics.harvard.edu

PERIMETER INSTITUTE FOR THEORETICAL PHYSICS

NSF

PHYSICS
VE RI TAS
HARVARD

Outline

1. Antiferromagnetism and quantum criticality in insulators

2. Onset of antiferromagnetism in metals, and d-wave superconductivity

3. Competing density wave order, and the pseudogap of the cuprate superconductors

4. Non-Fermi liquids

Outline

1. Antiferromagnetism and quantum criticality in insulators

2. Onset of antiferromagnetism in metals, and d-wave superconductivity

3. Competing density wave order, and the pseudogap of the cuprate superconductors

4. Non-Fermi liquids

Square lattice antiferromagnet

$$H = \sum_{\langle ij \rangle} J_{ij} \vec{S}_i \cdot \vec{S}_j$$

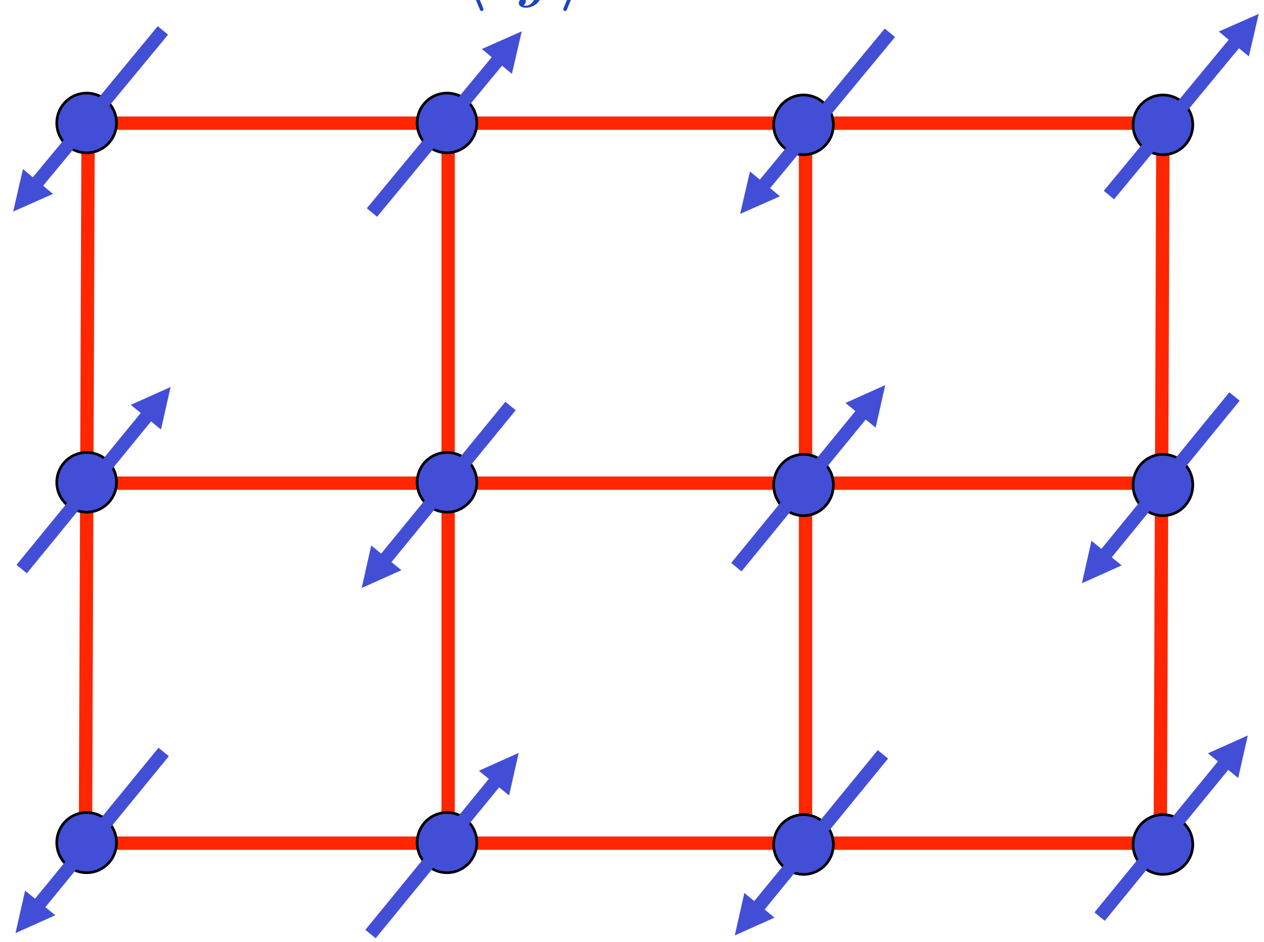

Ground state has long-range Néel order

Order parameter is a single vector field $\vec{\varphi} = \eta_i \vec{S}_i$

$\eta_i = \pm 1$ on two sublattices

$\langle \vec{\varphi} \rangle \neq 0$ in Néel state.

Square lattice antiferromagnet

$$H = \sum_{\langle ij \rangle} J_{ij} \vec{S}_i \cdot \vec{S}_j$$

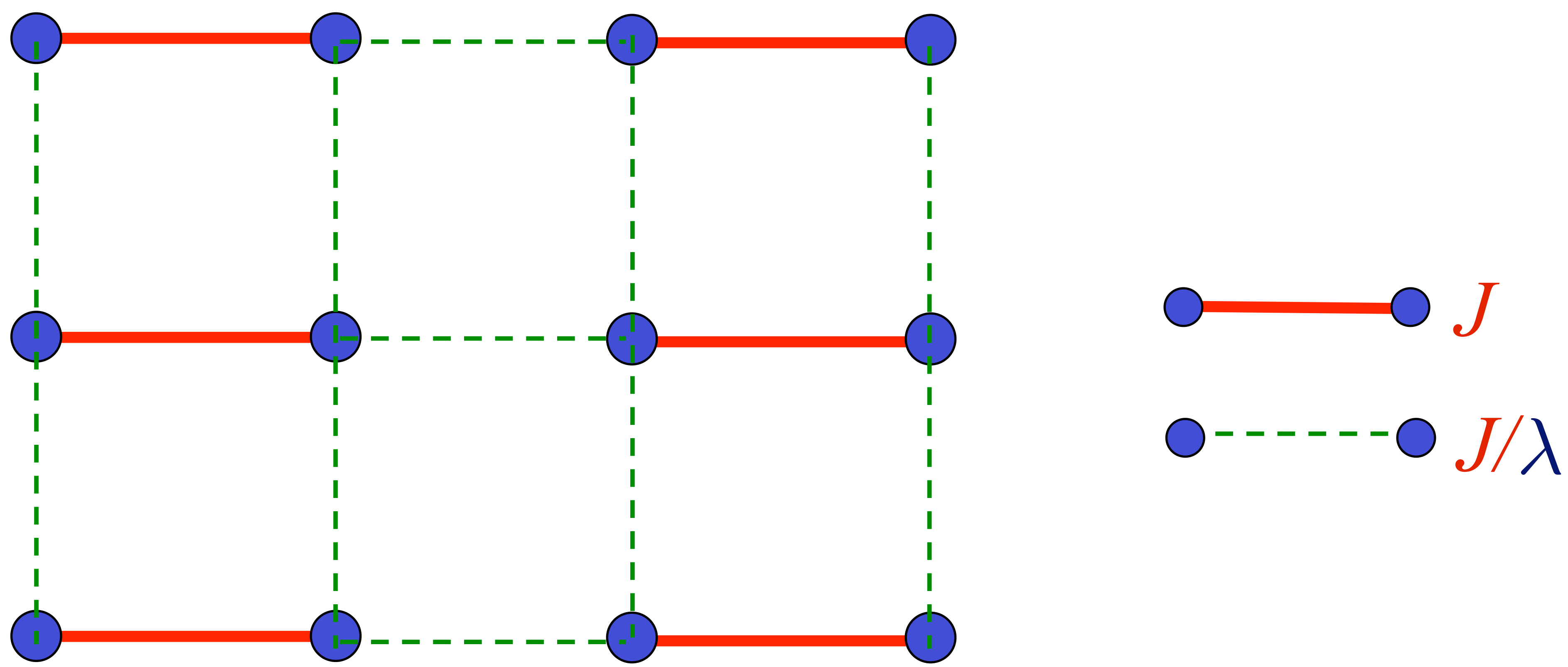

Weaken some bonds to induce spin entanglement in a new quantum phase

Square lattice antiferromagnet

$$H = \sum_{\langle ij \rangle} J_{ij} \vec{S}_i \cdot \vec{S}_j$$

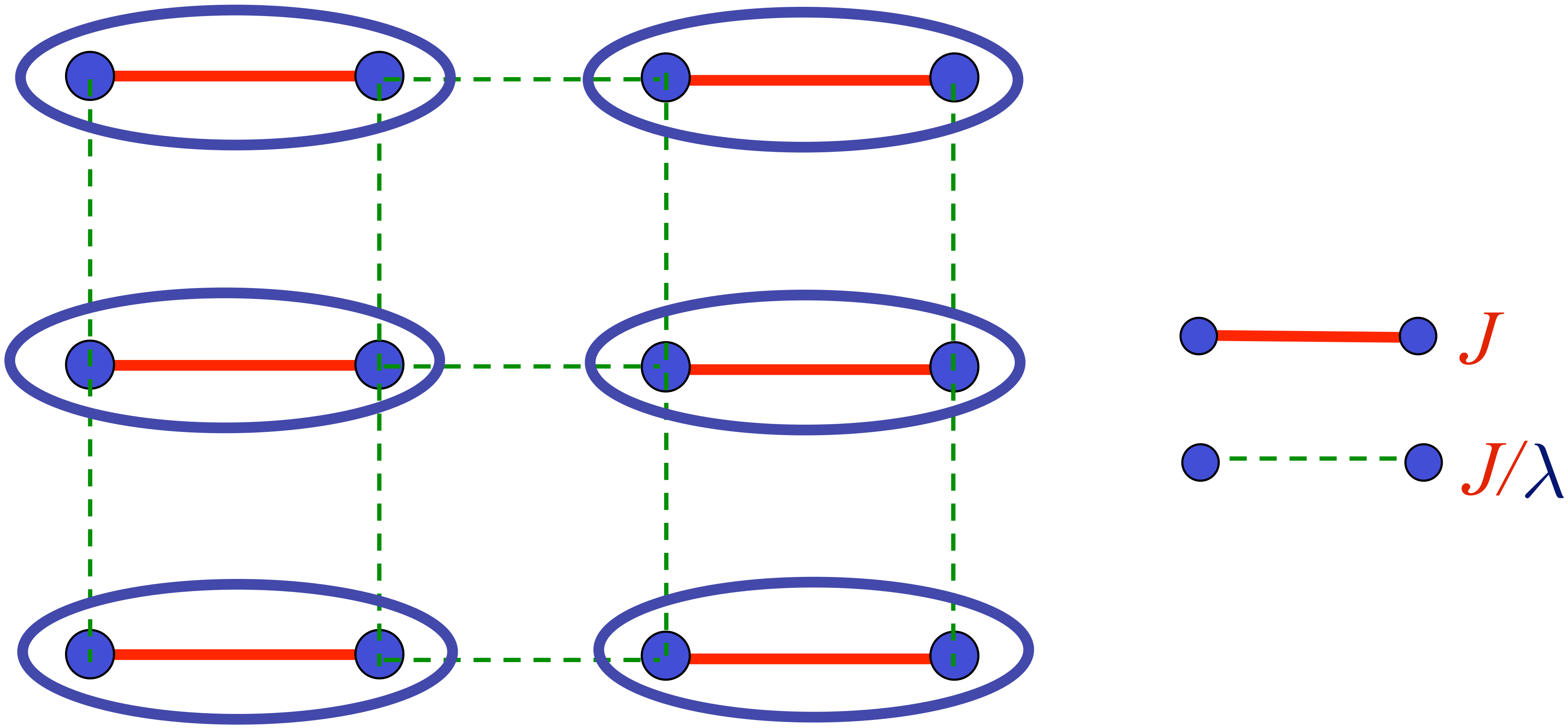

Ground state is a "quantum paramagnet" with spins locked in valence bond singlets

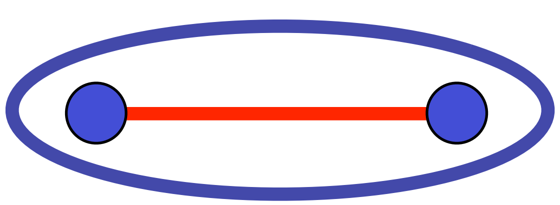

$$= \frac{1}{\sqrt{2}} \left(\left| \uparrow\downarrow \right\rangle - \left| \downarrow\uparrow \right\rangle \right)$$

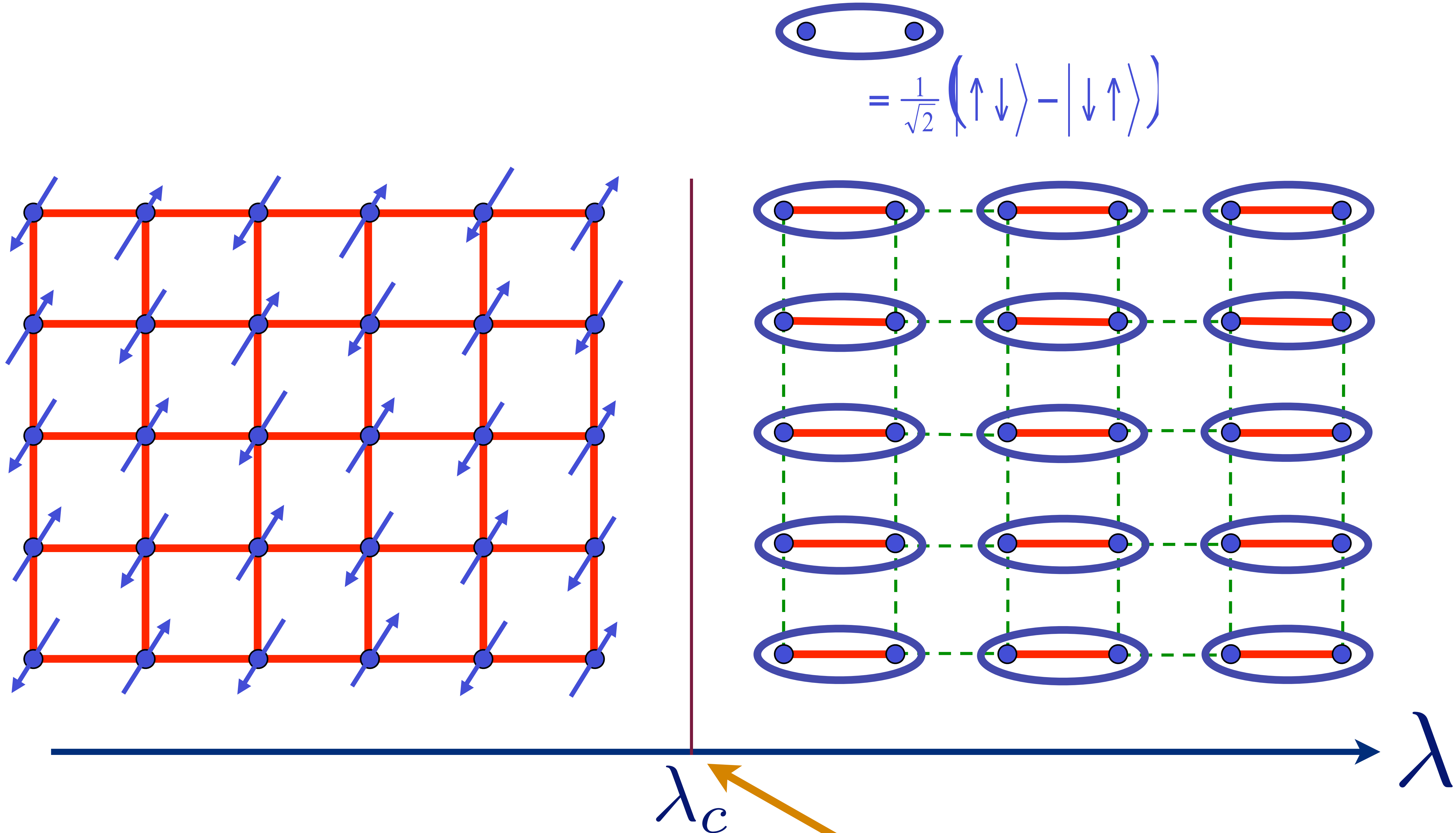

Quantum critical point with non-local entanglement in spin wavefunction

M. Matsumoto, C. Yasuda, S. Todo, and H. Takayama, *Phys. Rev.* B **65**, 014407 (2002).

Excitation spectrum in the paramagnetic phase

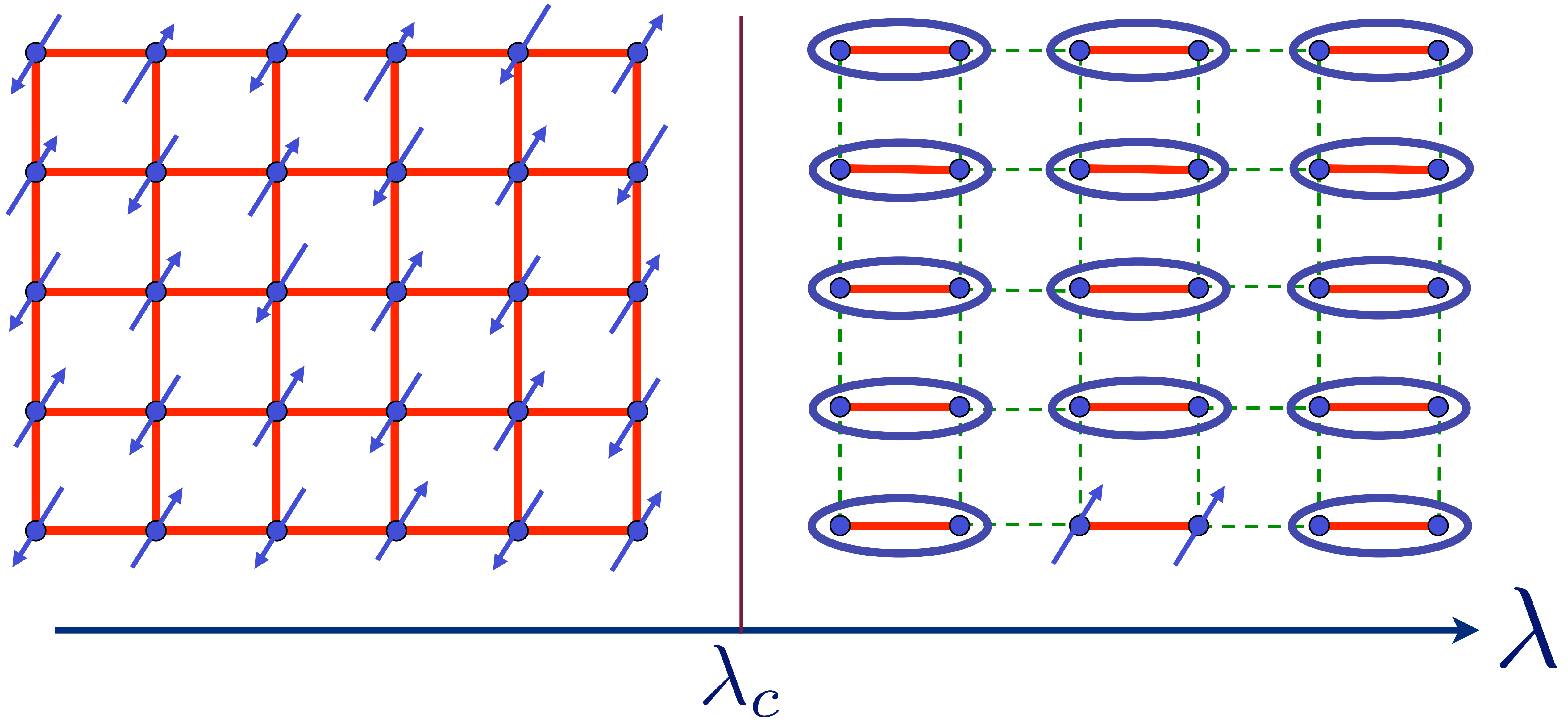

Excitation spectrum in the paramagnetic phase

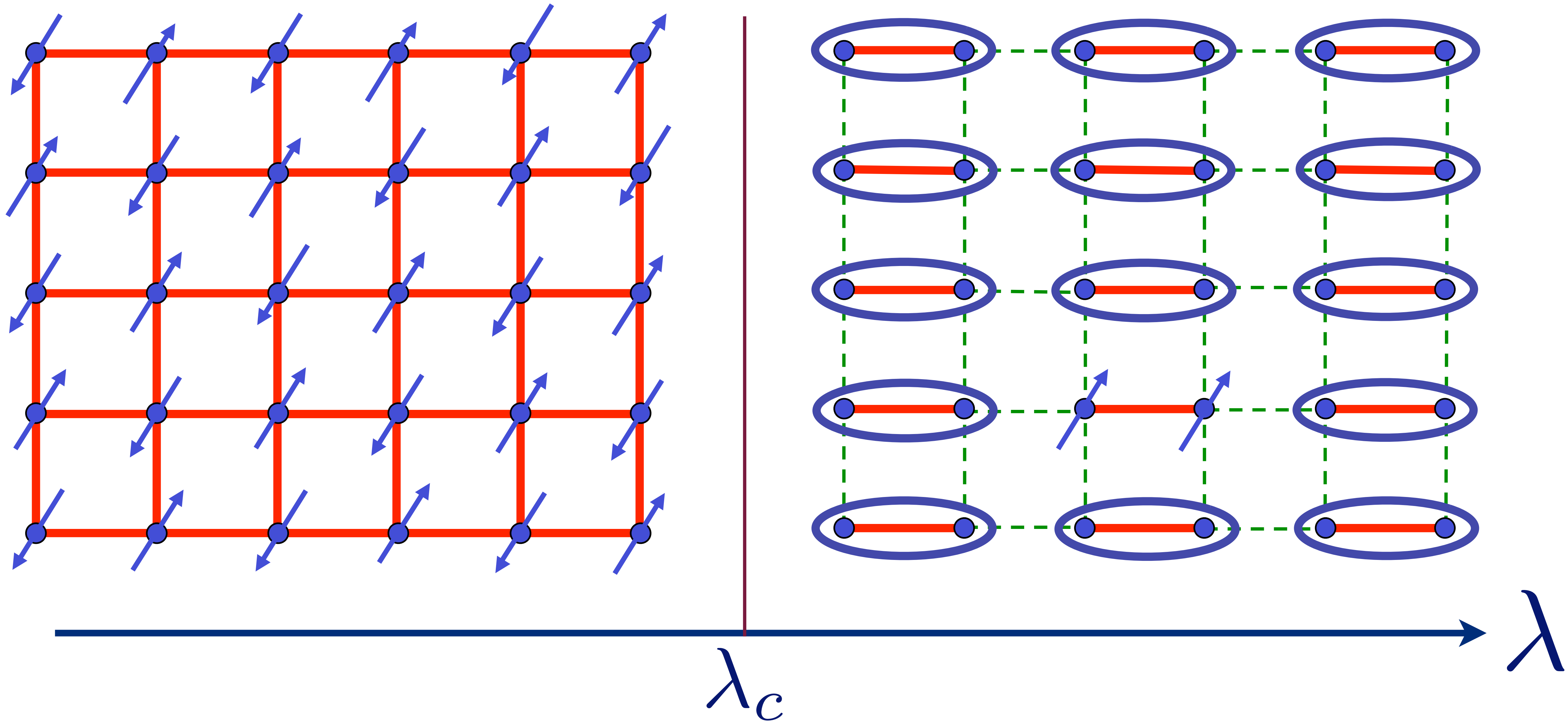

Excitation spectrum in the paramagnetic phase

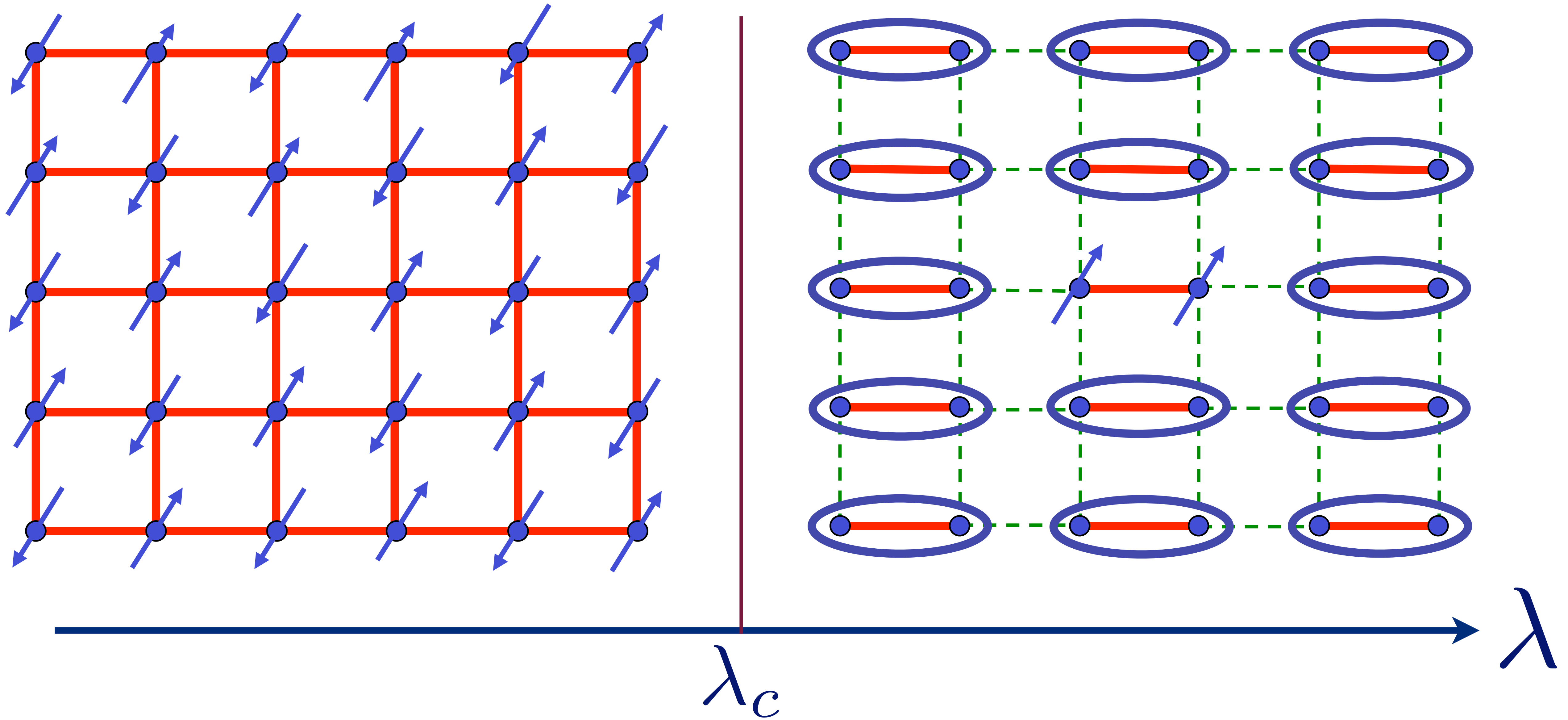

Excitation spectrum in the paramagnetic phase

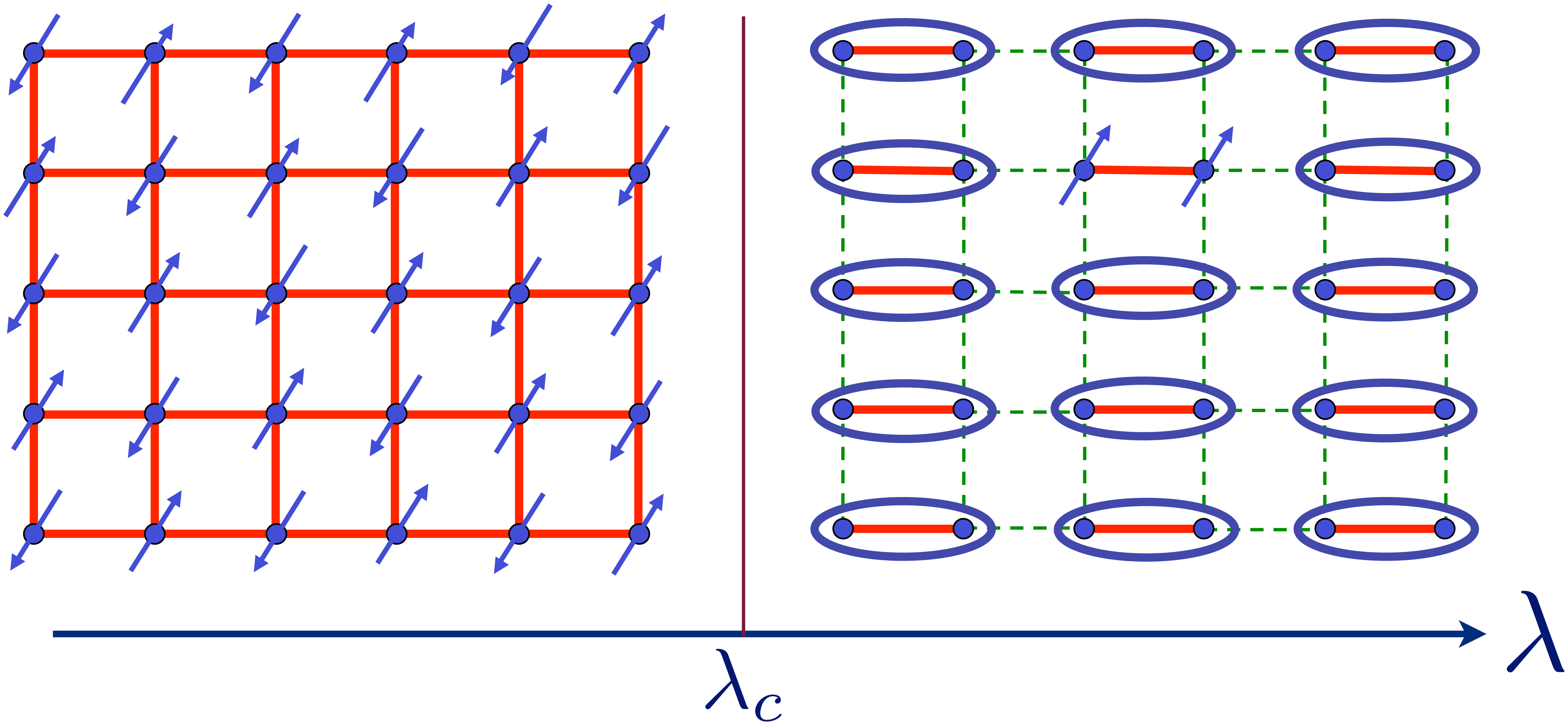

Excitation spectrum in the paramagnetic phase

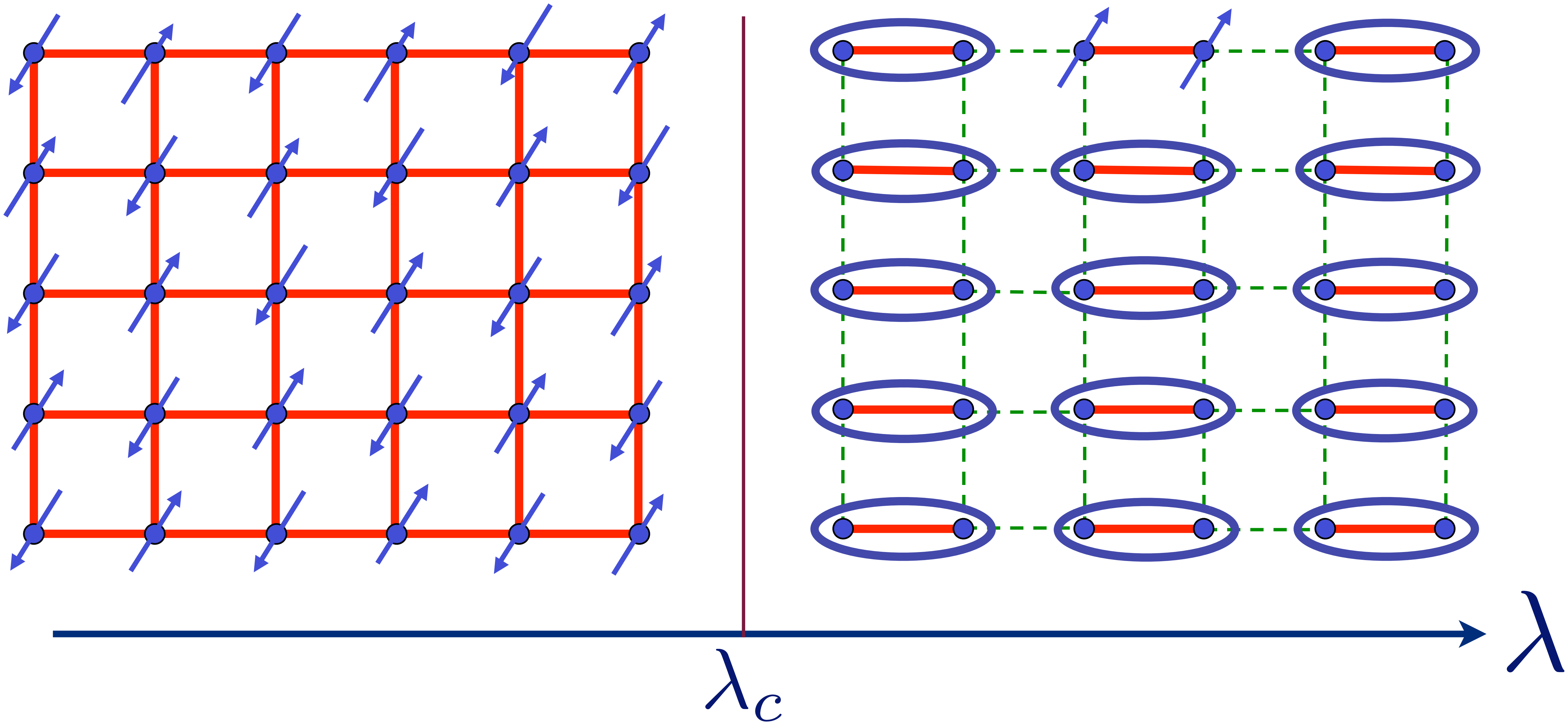

Sharp spin 1 particle excitation above an energy gap (spin gap)

Excitation spectrum in the Néel phase

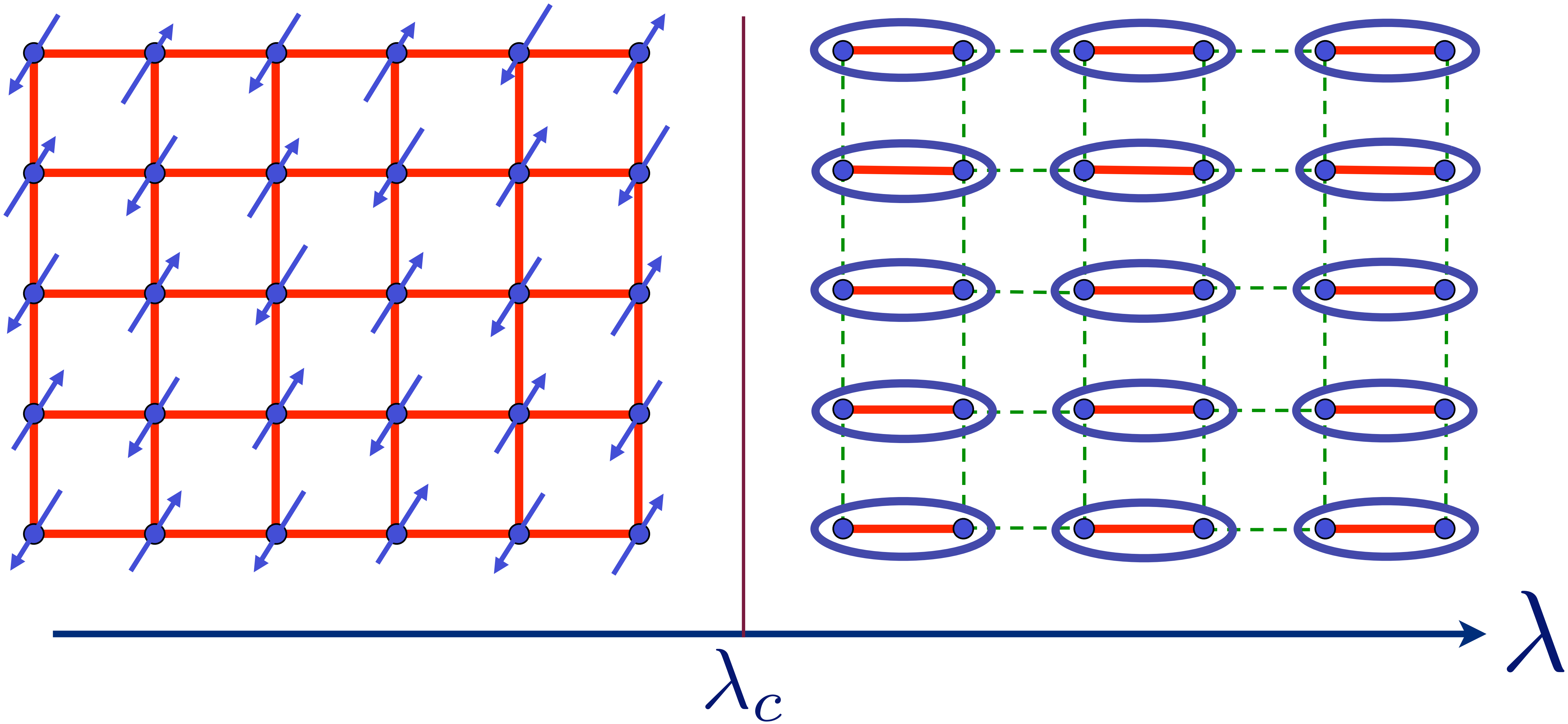

Excitation spectrum in the Néel phase

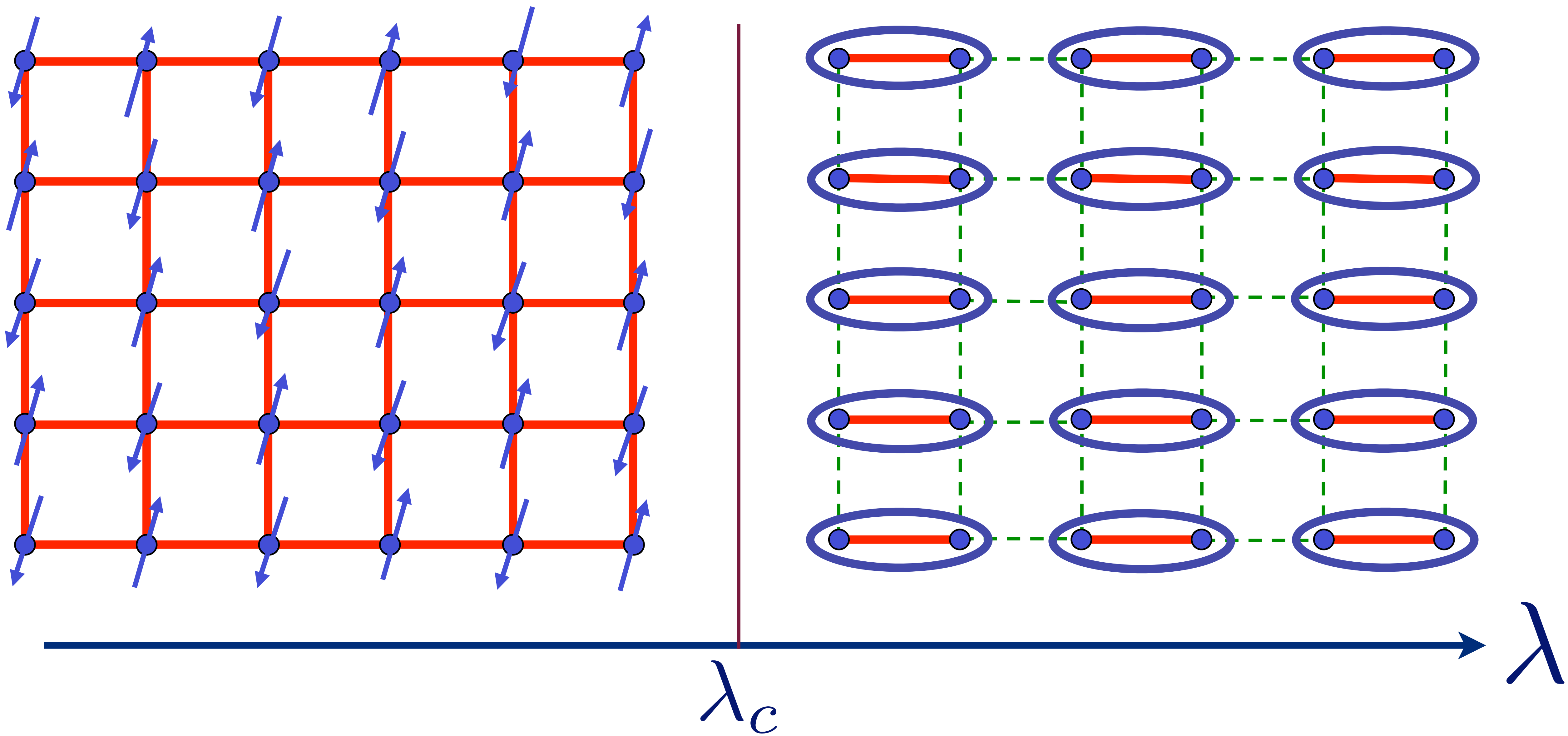

Spin waves

Excitation spectrum in the Néel phase

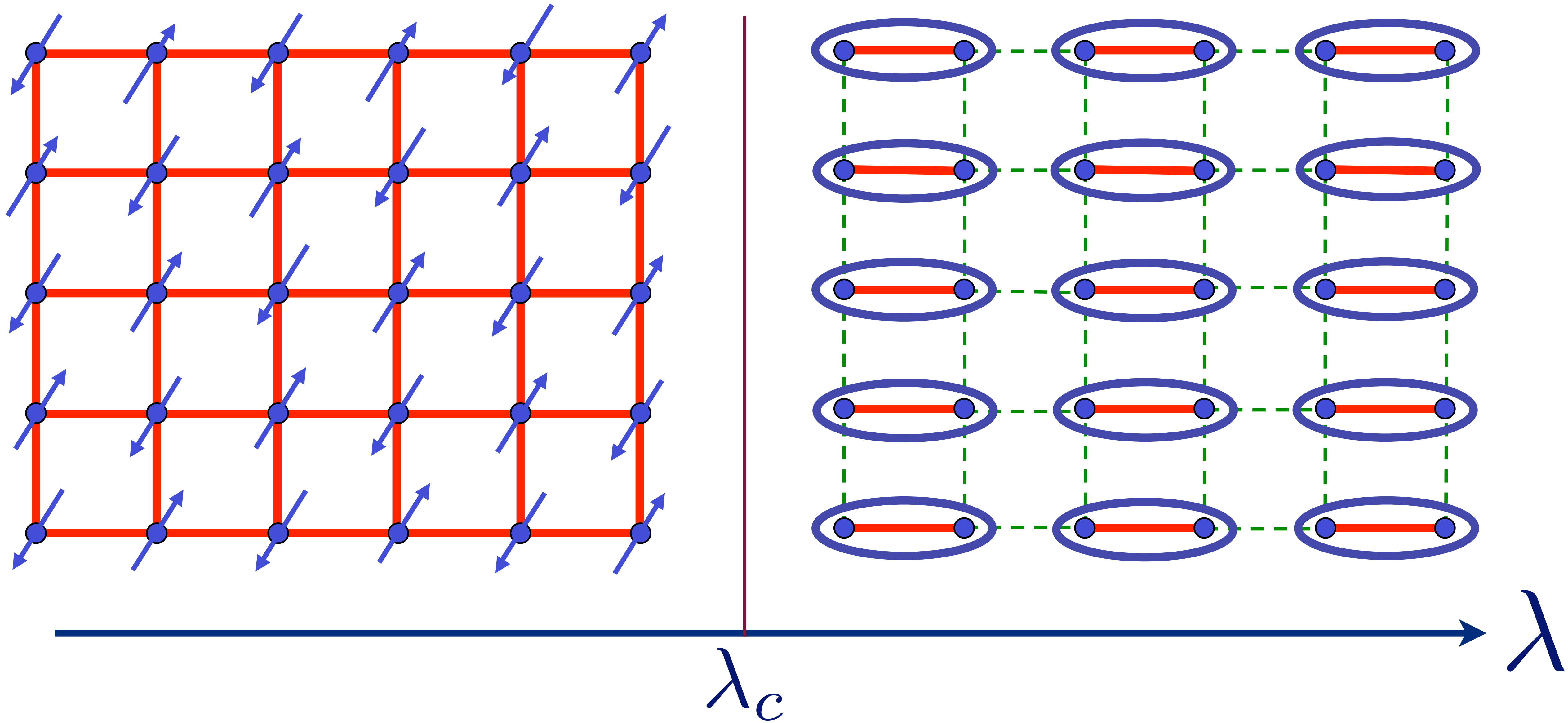

Spin waves

Derivation of field theory of critical point

Description using Landau-Ginzburg field theory

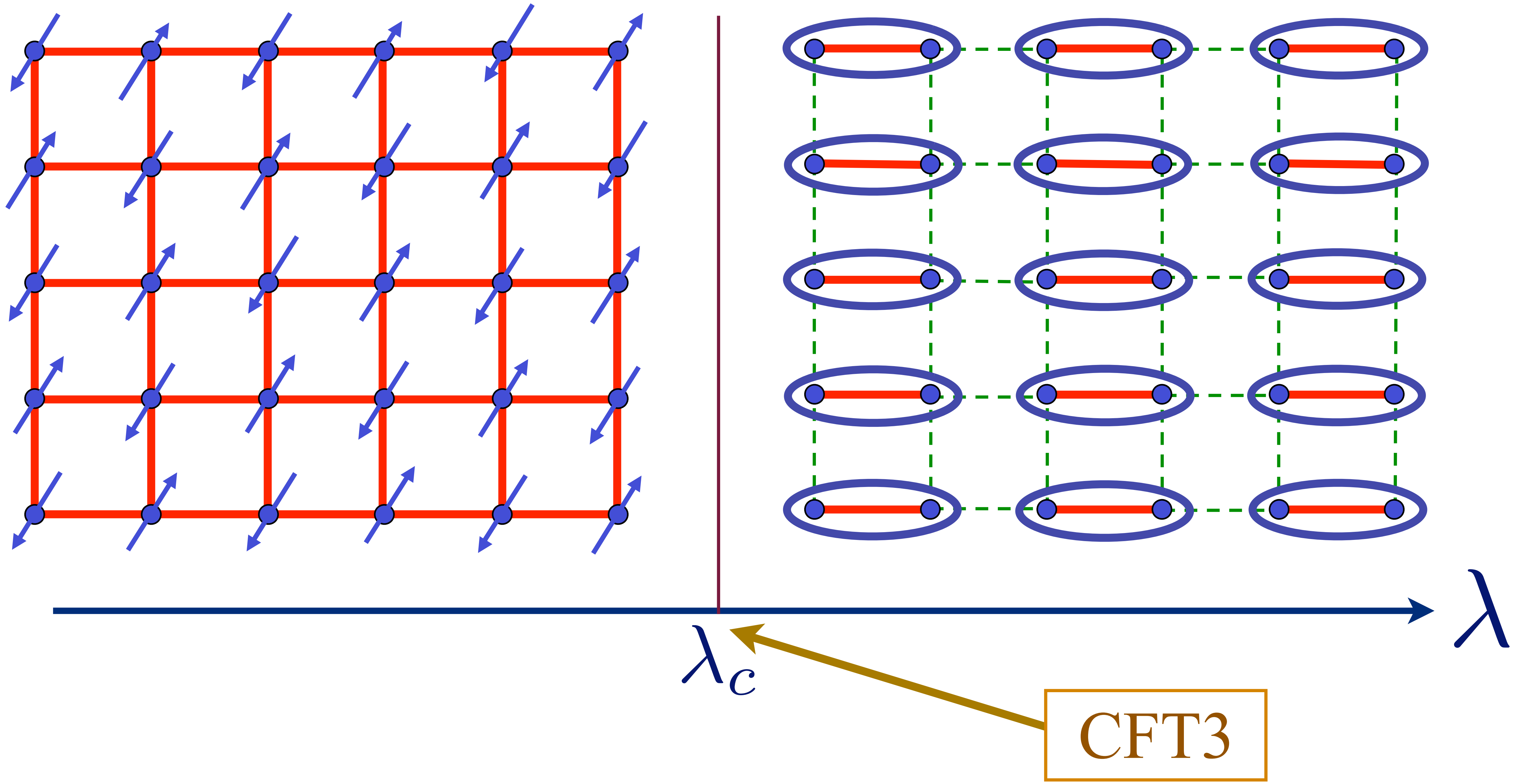

O(3) order parameter $\vec{\varphi}$

$$\mathcal{S} = \int d^2r d\tau \left[(\partial_\tau \varphi)^2 + c^2 (\nabla_r \vec{\varphi})^2 + (\lambda - \lambda_c)\vec{\varphi}^2 + u \left(\vec{\varphi}^2\right)^2 \right]$$

Excitation spectrum in the paramagnetic phase

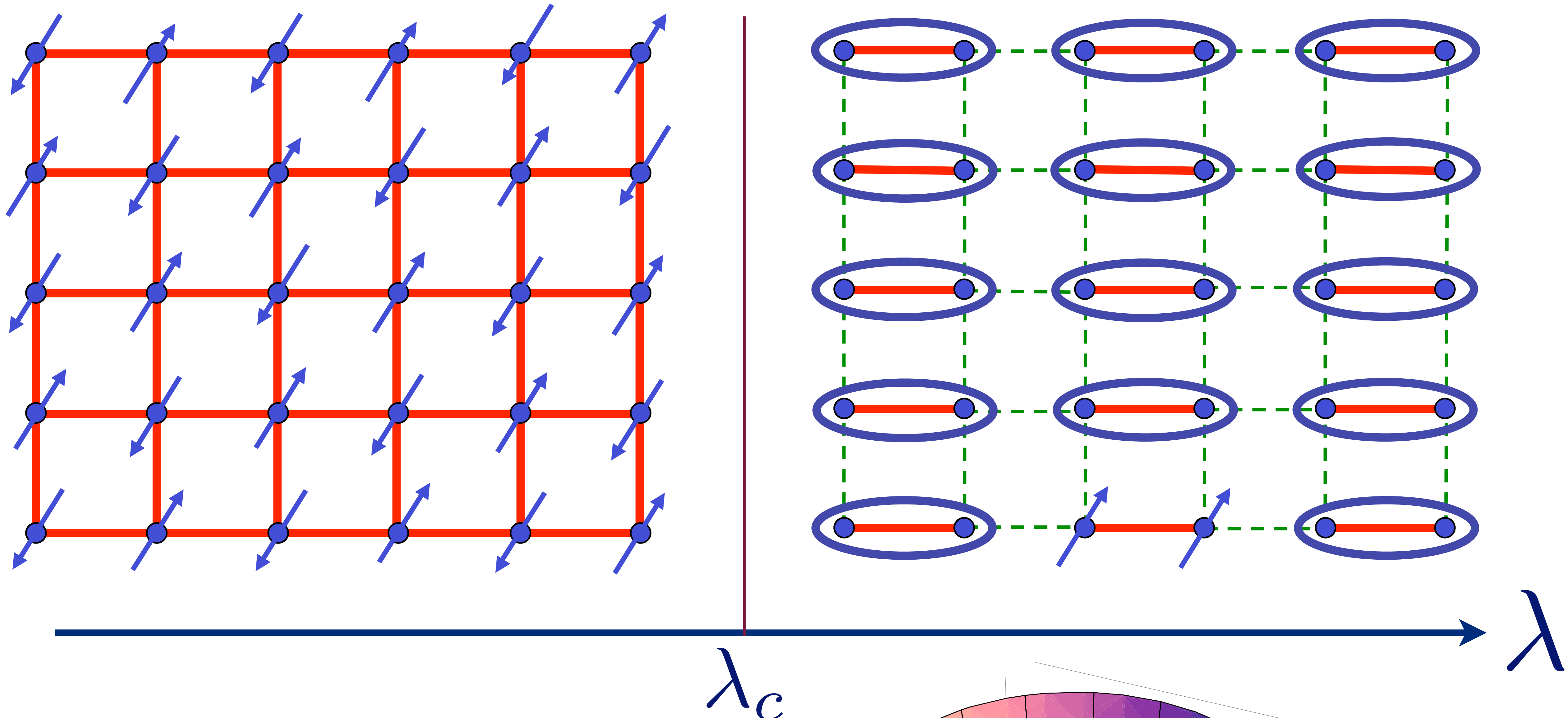

$$V(\vec{\varphi}) = (\lambda - \lambda_c)\vec{\varphi}^2 + u\left(\vec{\varphi}^2\right)^2$$

$$\lambda > \lambda_c$$

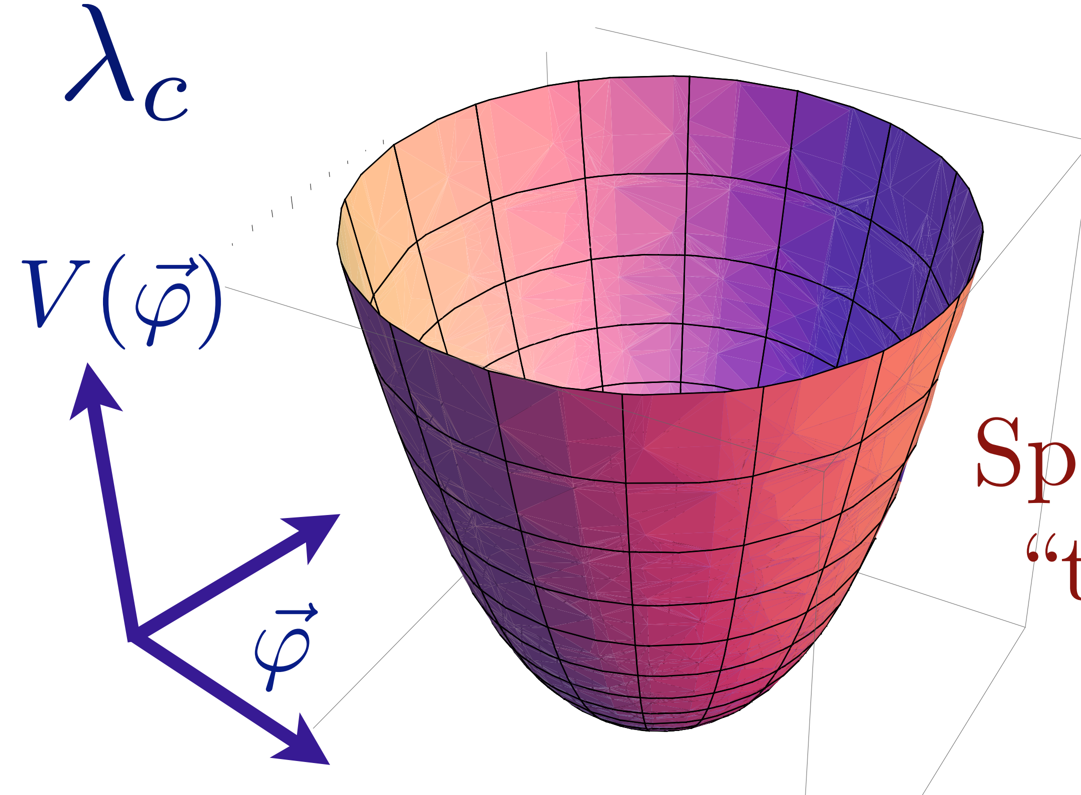

Spin $S = 1$
"triplon"

Excitation spectrum in the paramagnetic phase

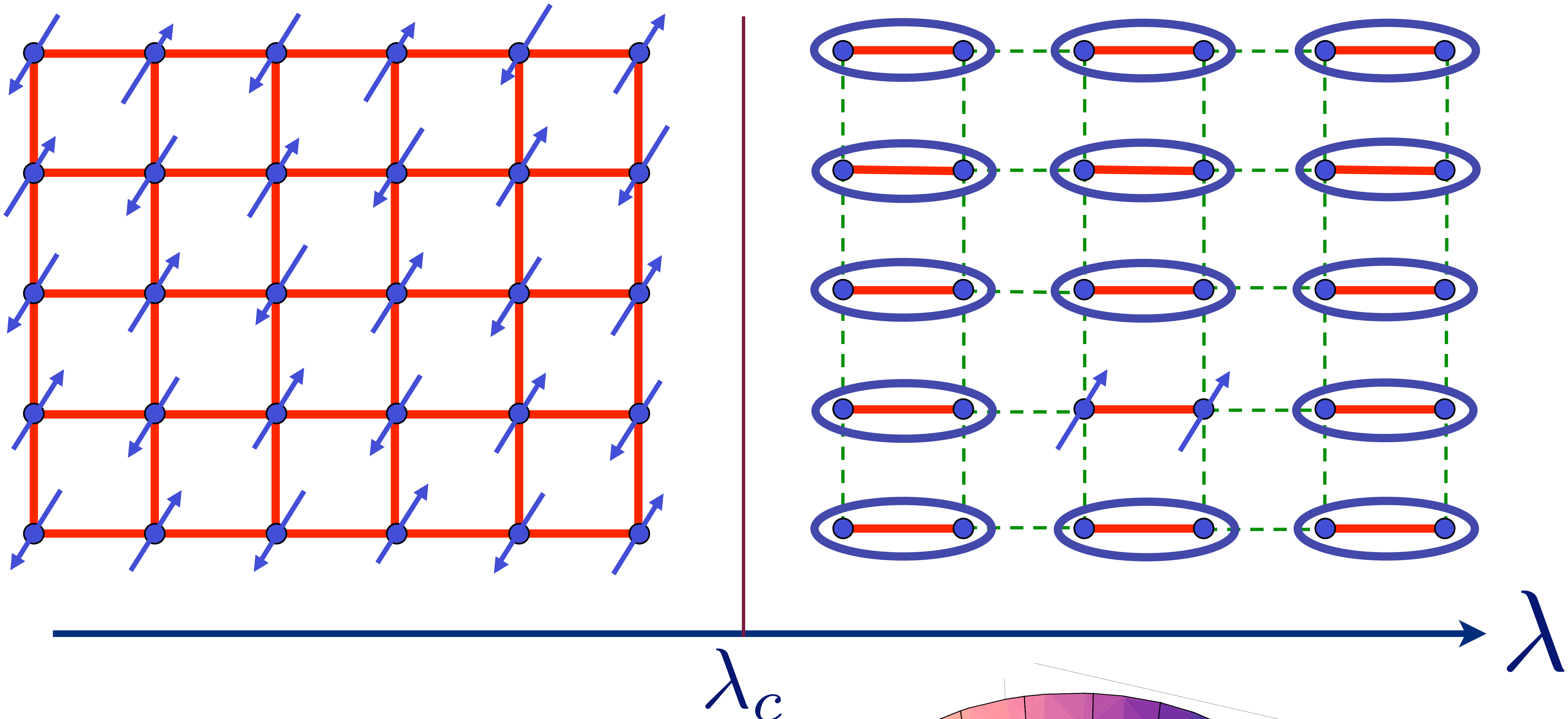

$$V(\vec{\varphi}) = (\lambda - \lambda_c)\vec{\varphi}^2 + u\left(\vec{\varphi}^2\right)^2$$

$$\lambda > \lambda_c$$

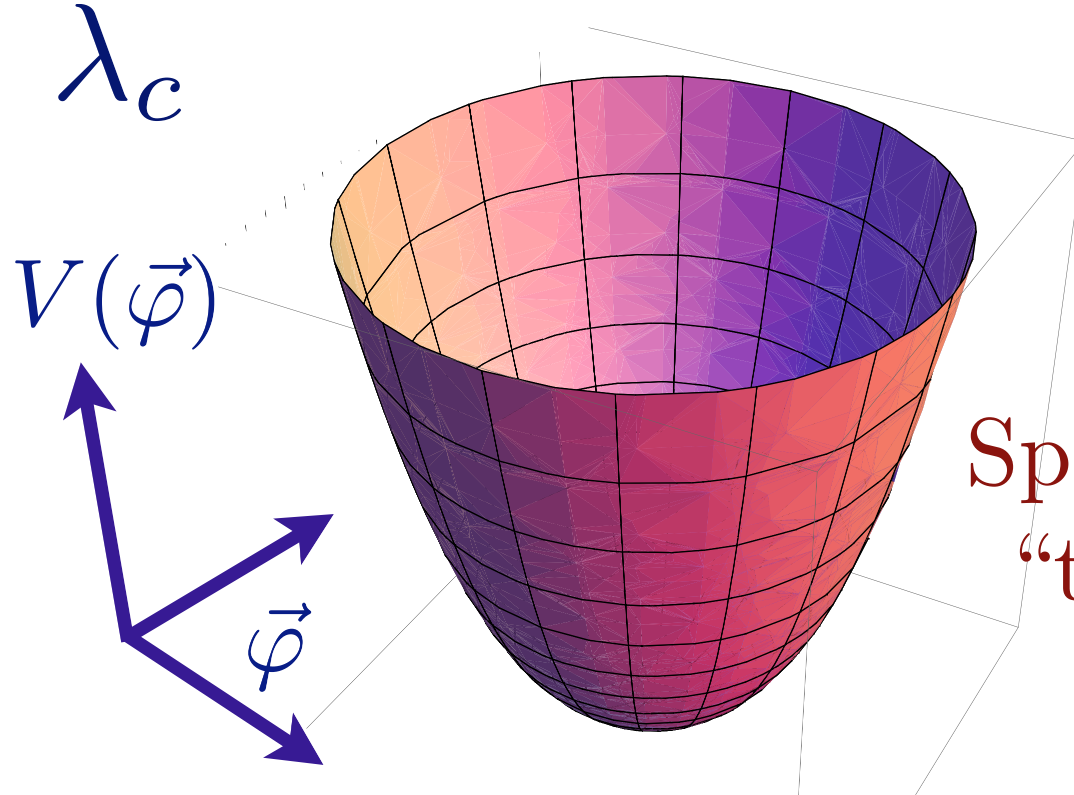

Spin $S = 1$
"triplon"

Excitation spectrum in the paramagnetic phase

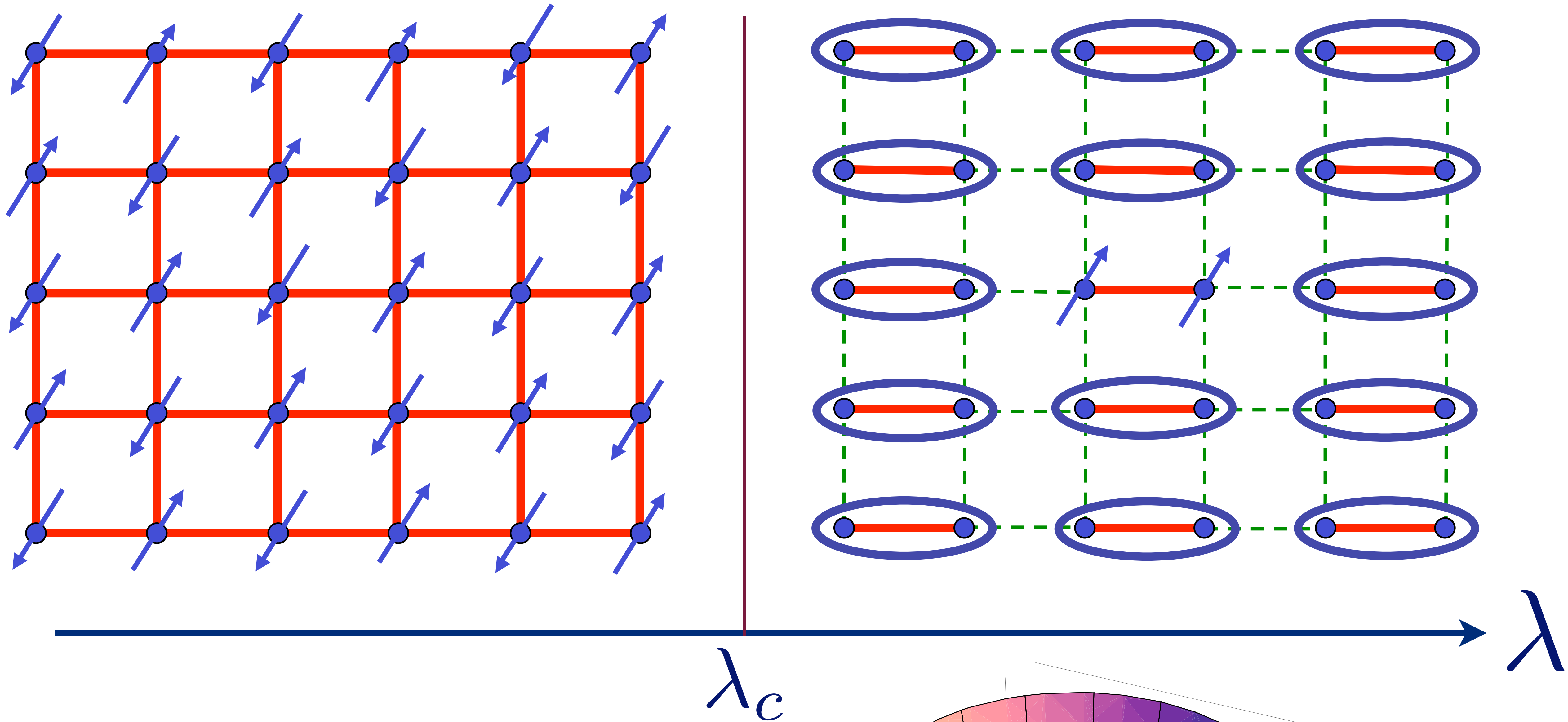

$$V(\vec{\varphi}) = (\lambda - \lambda_c)\vec{\varphi}^2 + u\left(\vec{\varphi}^2\right)^2$$

$$\lambda > \lambda_c$$

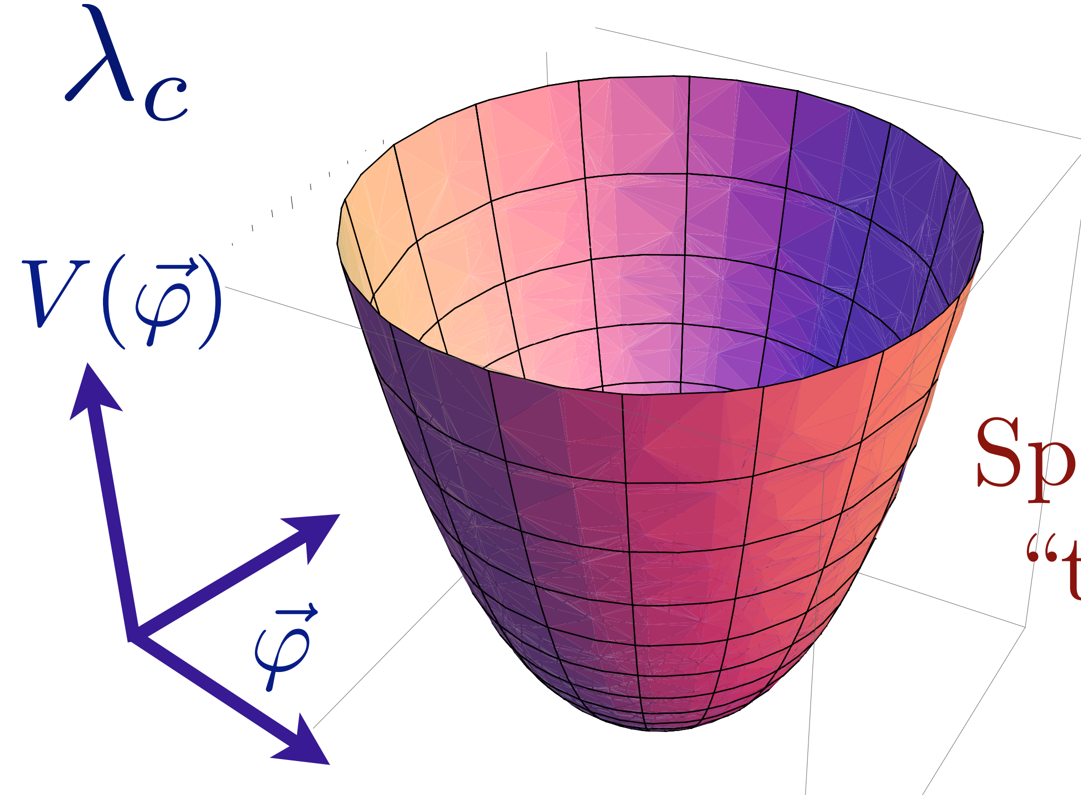

Spin $S = 1$
"triplon"

Excitation spectrum in the paramagnetic phase

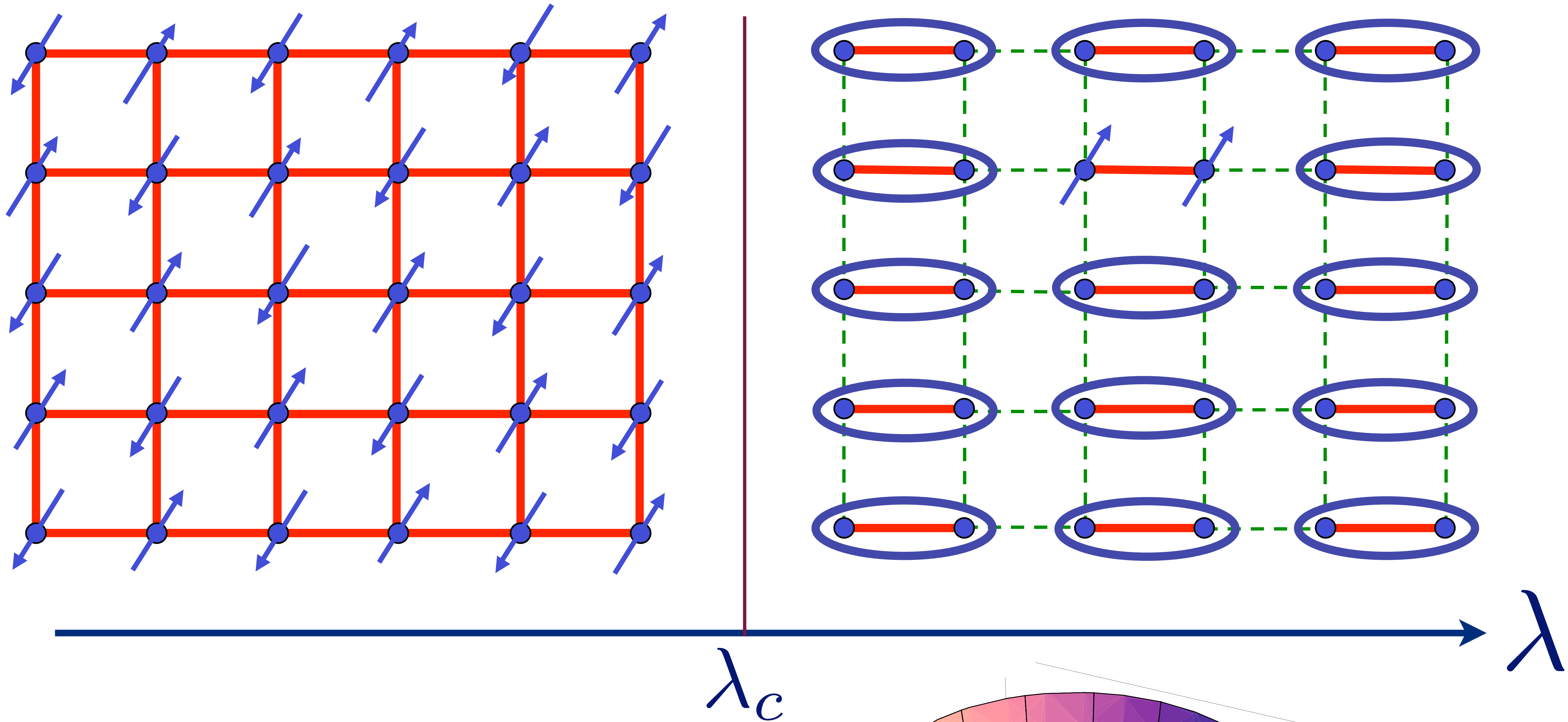

$$V(\vec{\varphi}) = (\lambda - \lambda_c)\vec{\varphi}^2 + u\left(\vec{\varphi}^2\right)^2$$

$$\lambda > \lambda_c$$

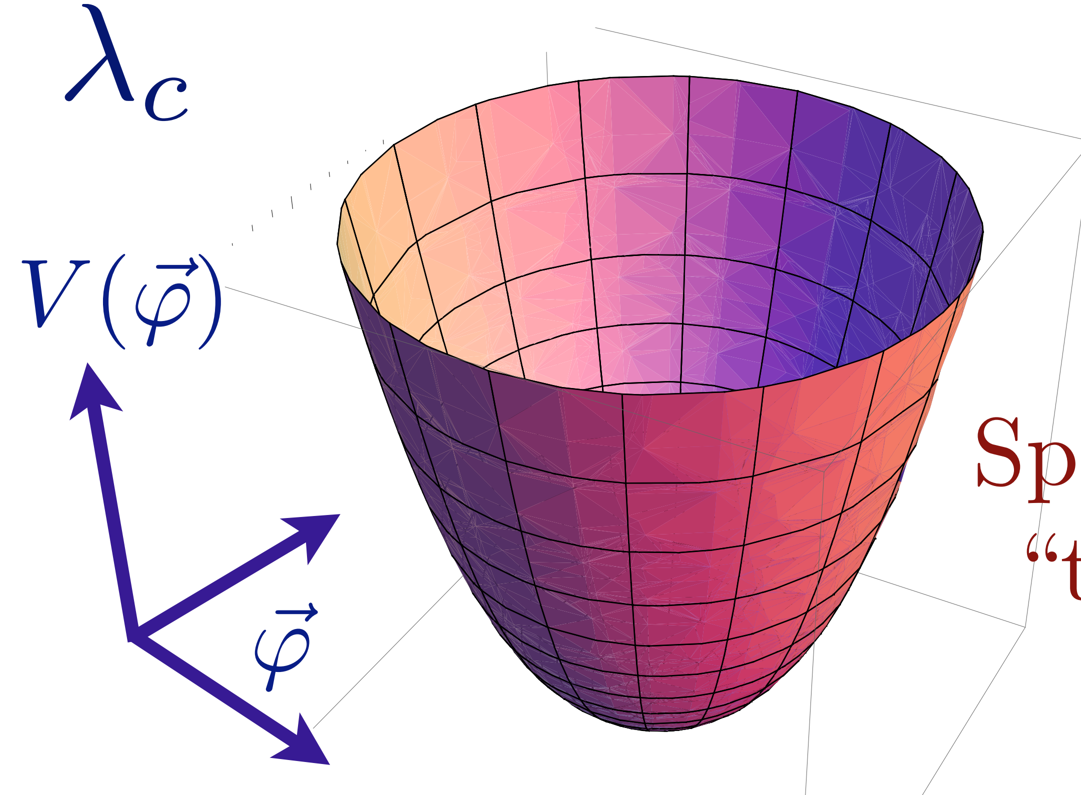

Spin $S = 1$
"triplon"

Excitation spectrum in the paramagnetic phase

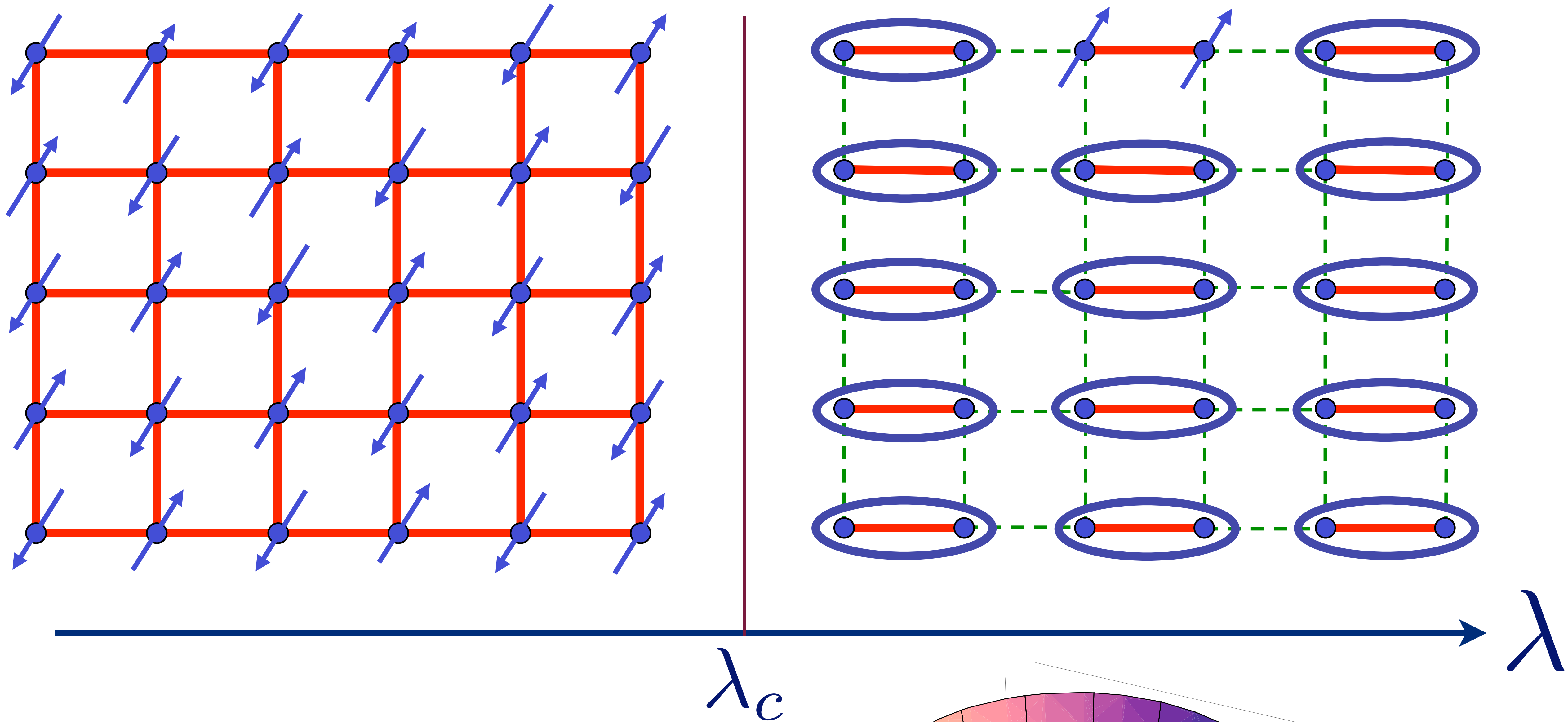

$$V(\vec{\varphi}) = (\lambda - \lambda_c)\vec{\varphi}^2 + u\left(\vec{\varphi}^2\right)^2$$

$$\lambda > \lambda_c$$

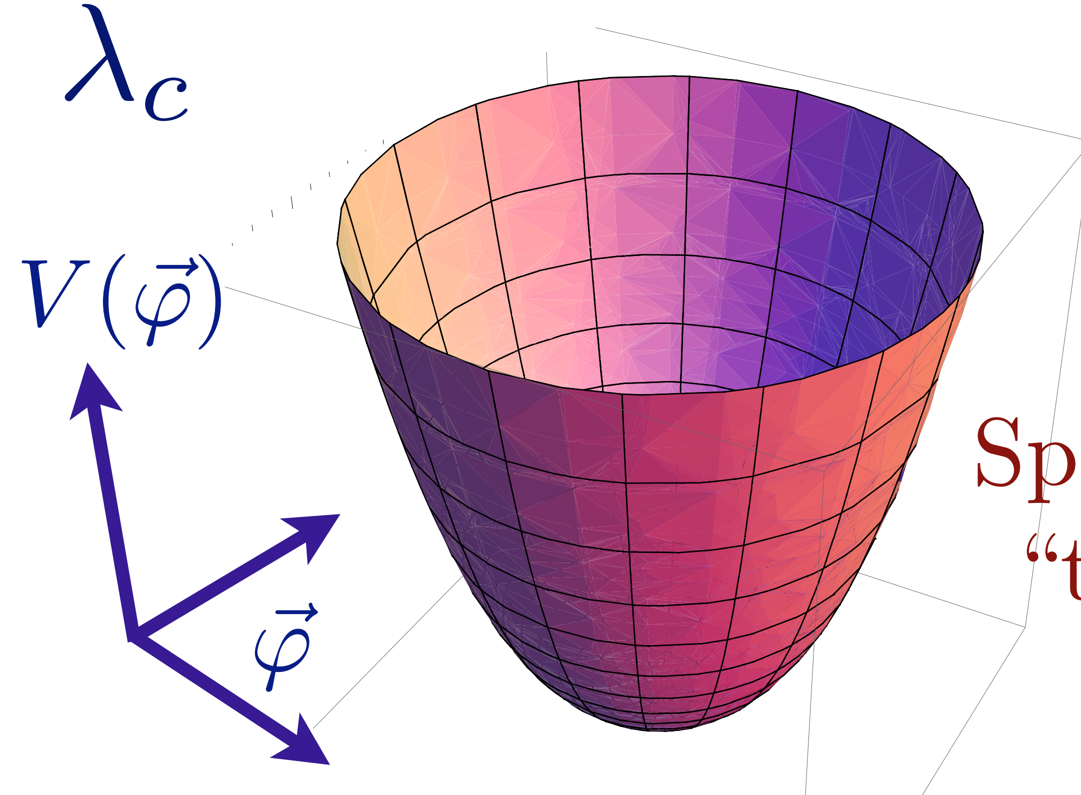

Spin $S = 1$
"triplon"

Excitation spectrum in the Néel phase

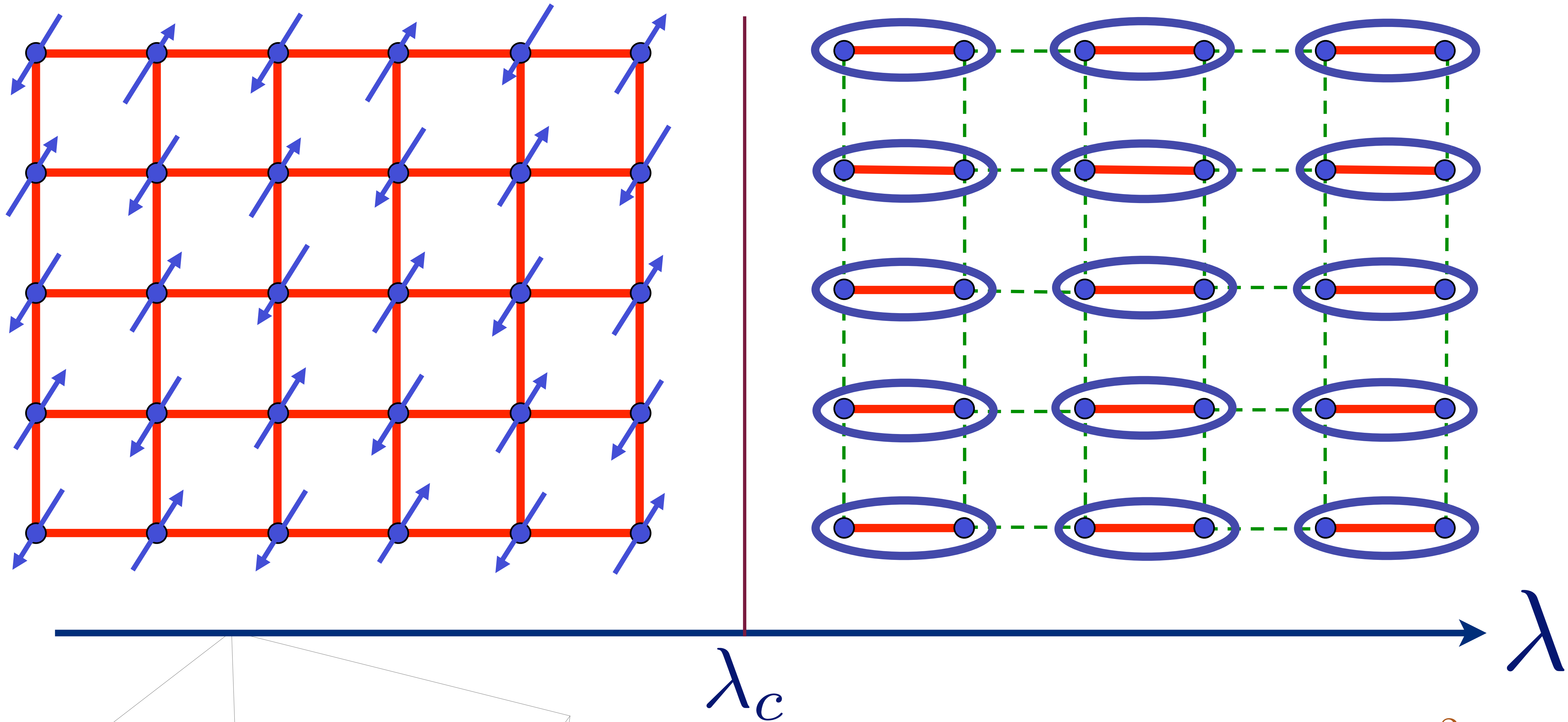

$$V(\vec{\varphi}) = (\lambda - \lambda_c)\vec{\varphi}^2 + u\left(\vec{\varphi}^2\right)^2$$

$$\lambda < \lambda_c$$

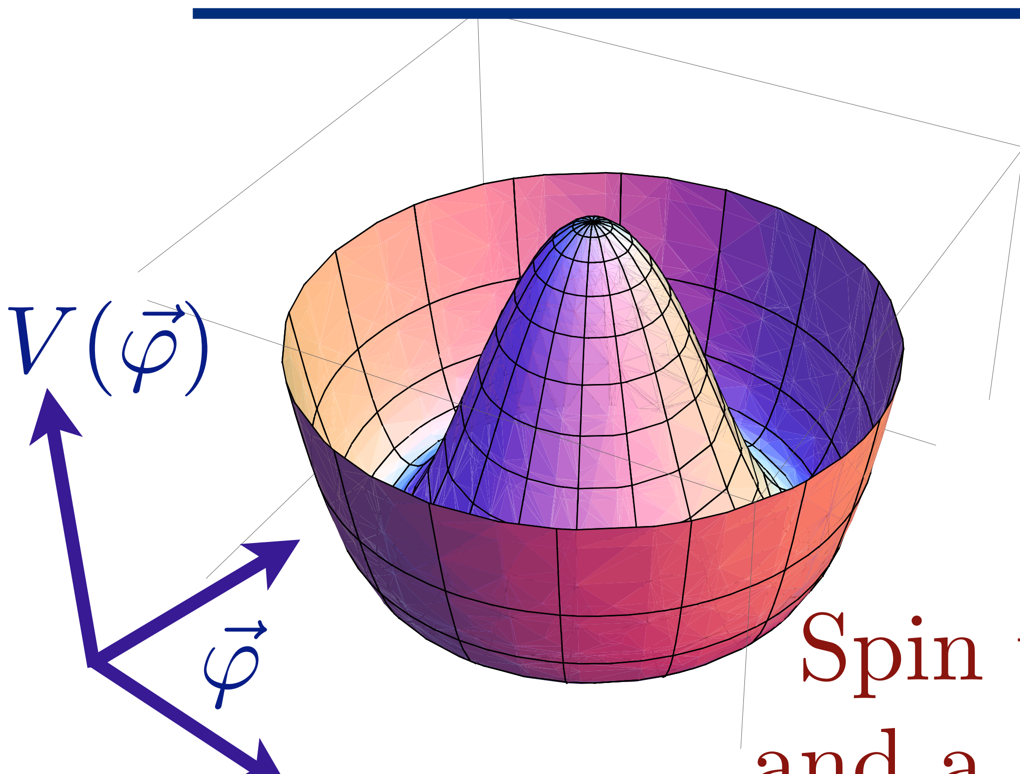

Spin waves (“Goldstone” modes) and a longitudinal “Higgs” particle

Excitation spectrum in the Néel phase

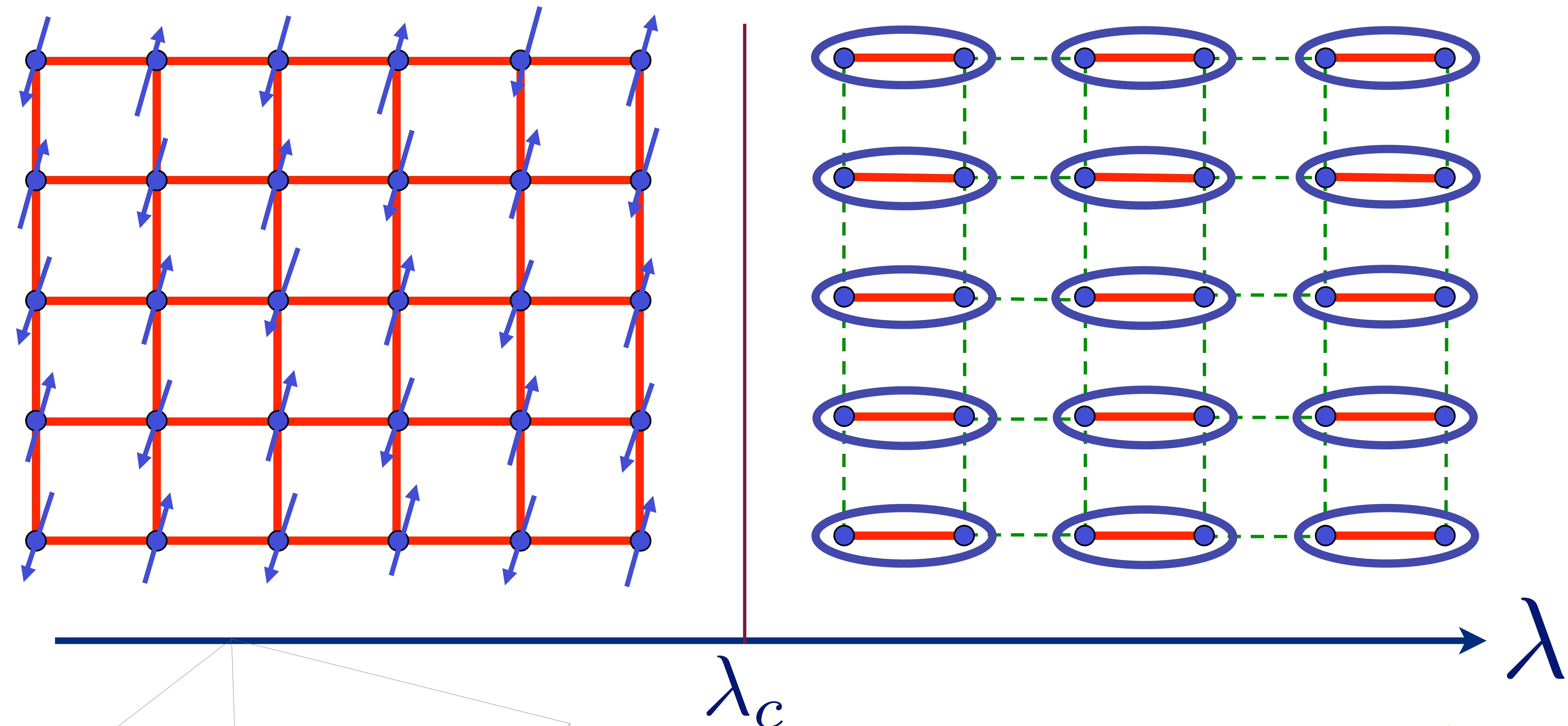

$$V(\vec{\varphi}) = (\lambda - \lambda_c)\vec{\varphi}^2 + u\left(\vec{\varphi}^2\right)^2$$

$$\lambda < \lambda_c$$

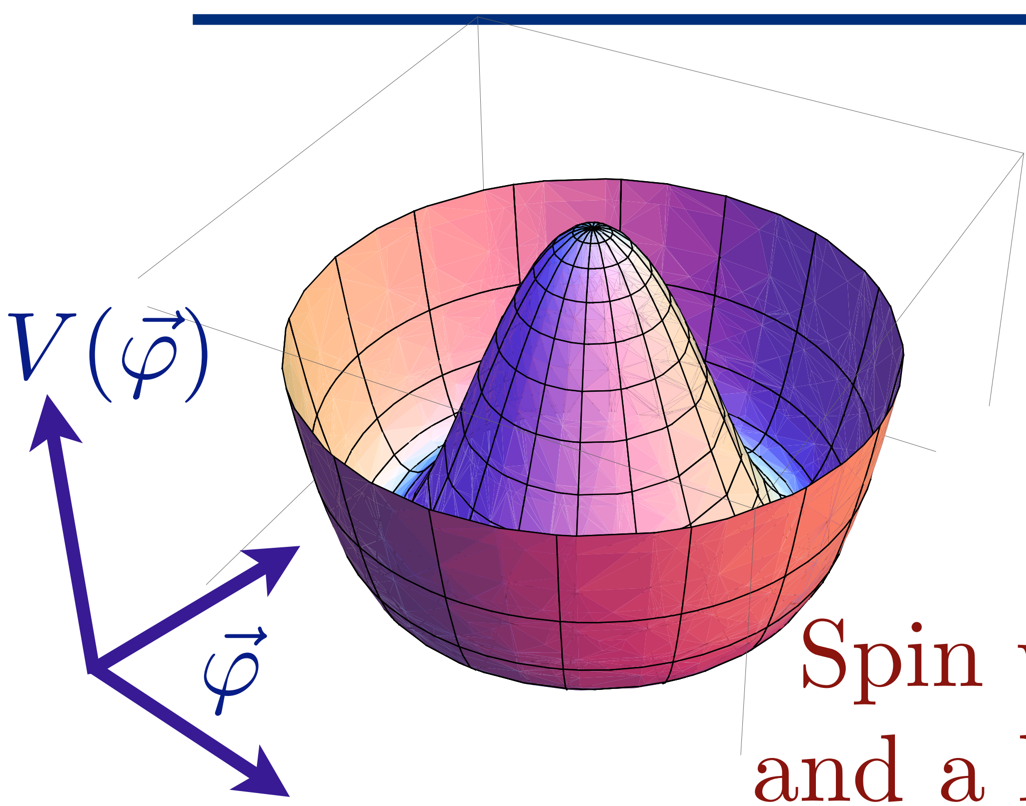

Spin waves (“Goldstone” modes) and a longitudinal “Higgs” particle

Excitation spectrum in the Néel phase

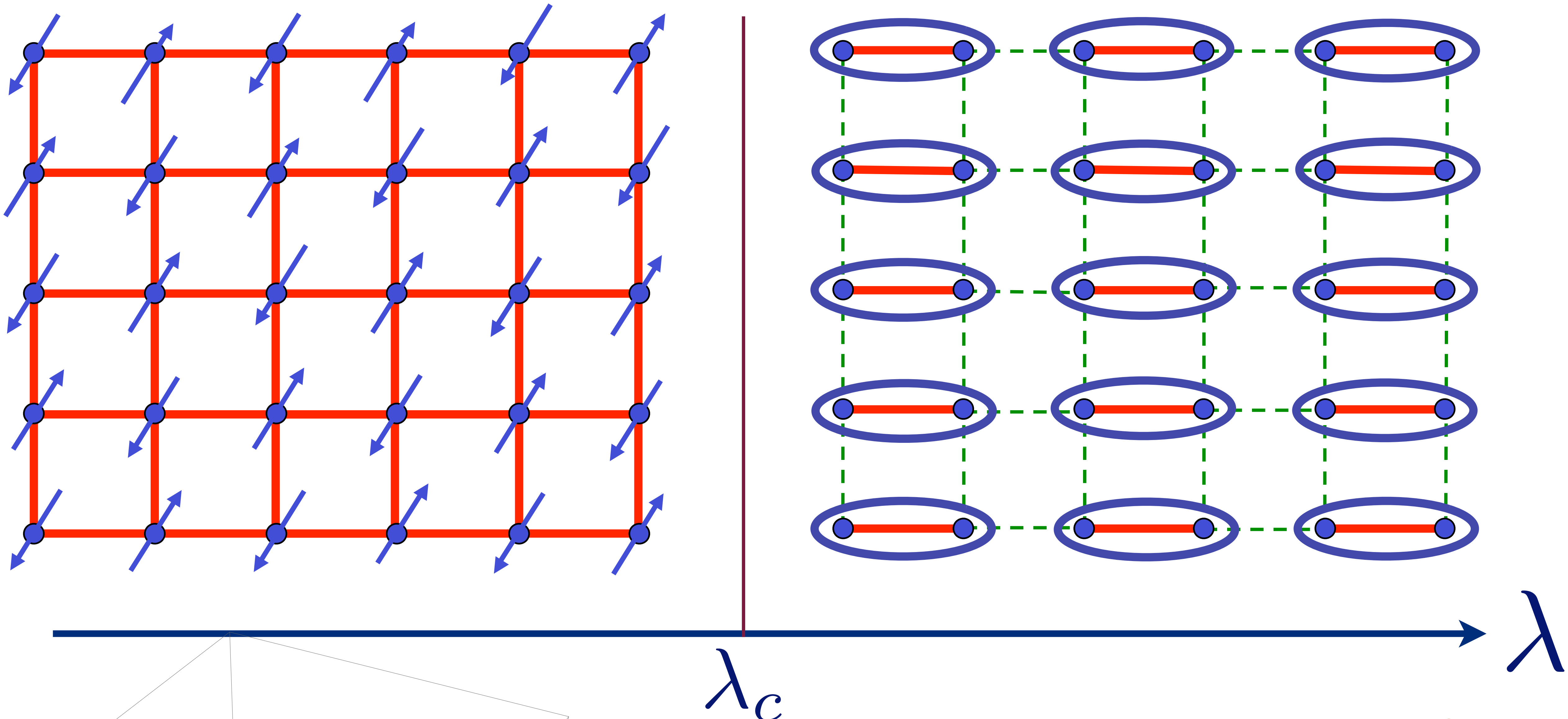

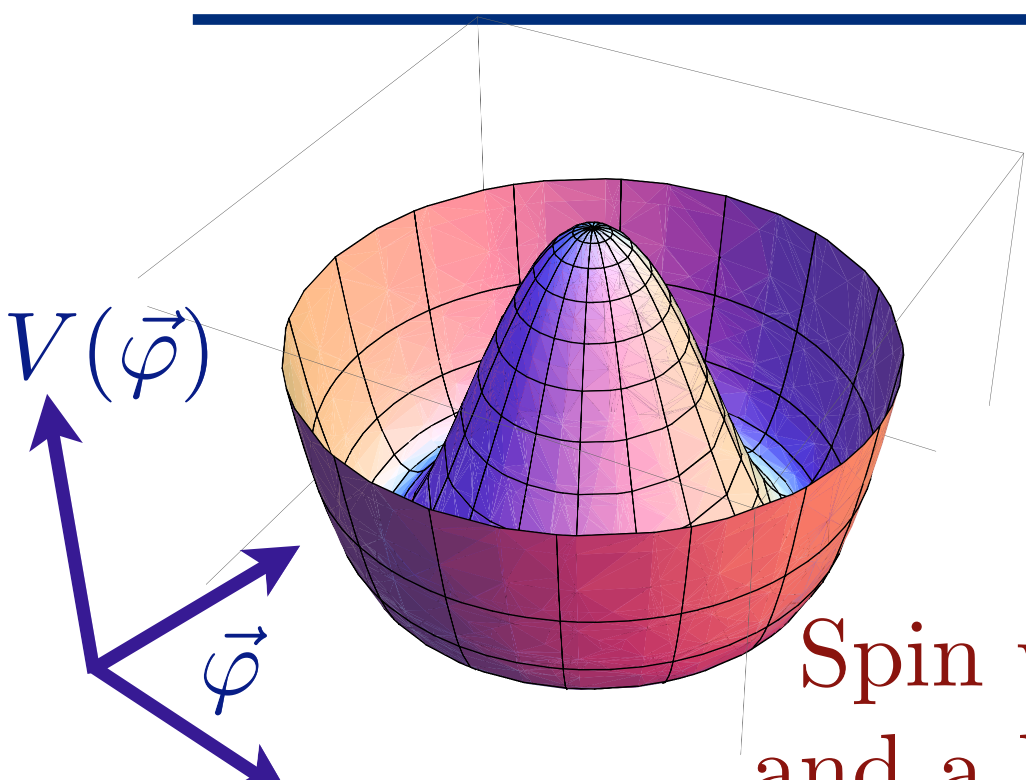

$$V(\vec{\varphi}) = (\lambda - \lambda_c)\vec{\varphi}^2 + u\left(\vec{\varphi}^2\right)^2$$

$$\lambda < \lambda_c$$

Spin waves ("Goldstone" modes)
and a longitudinal "Higgs" particle

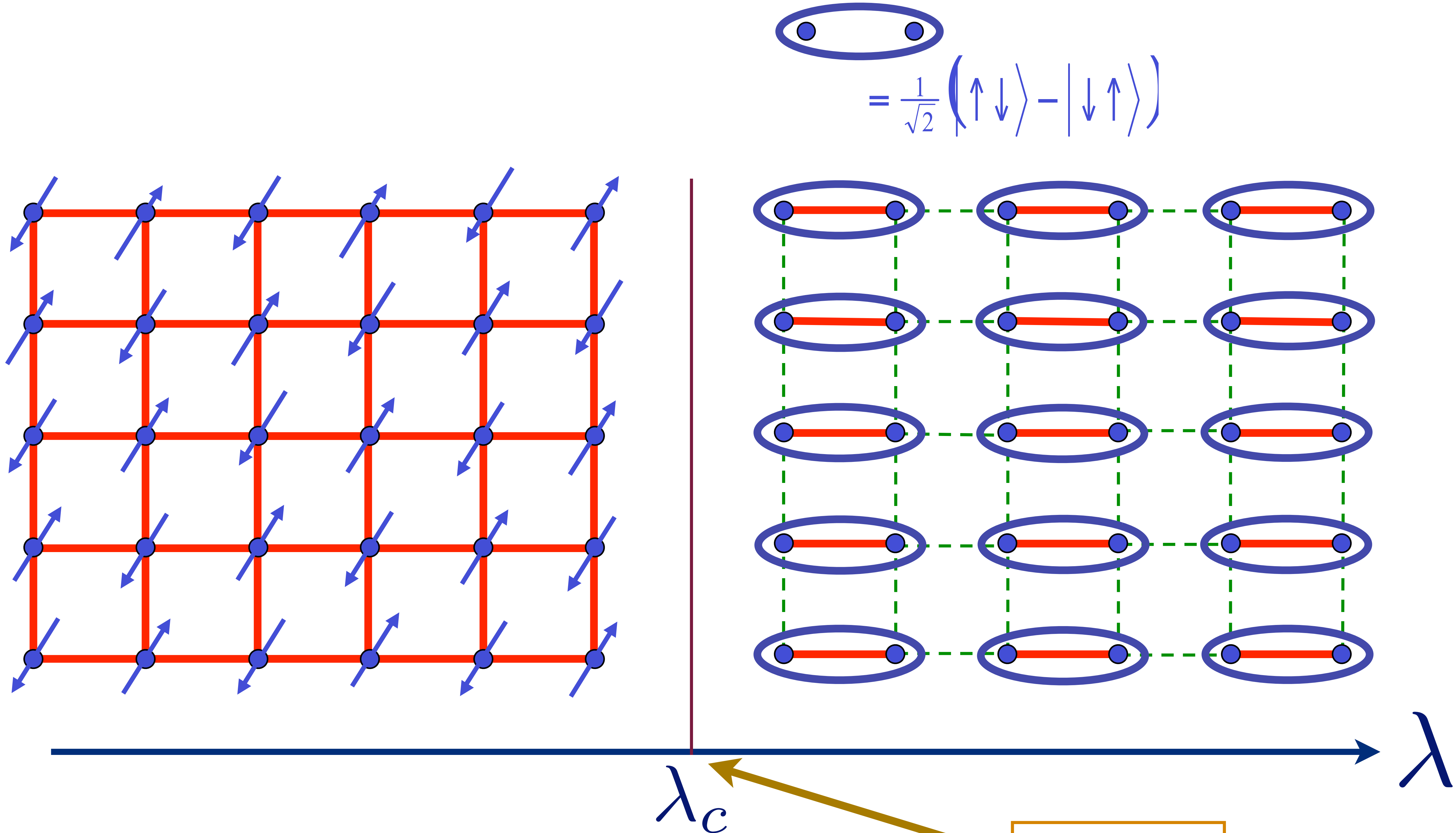

O(3) order parameter $\vec{\varphi}$

$$\mathcal{S} = \int d^2 r d\tau \left[(\partial_\tau \varphi)^2 + c^2 (\nabla_r \vec{\varphi})^2 + s\vec{\varphi}^2 + u\left(\vec{\varphi}^2\right)^2 \right]$$

Quantum Monte Carlo - critical exponents

Table IV: Fit results for the critical exponents ν, β/ν, and η. We summarize results including a variation of the critical point within its error bar. For the ladder model (top group of values) fit results and quality of fits are also given at the previous best estimate of α_c. The bottom group are results for the plaquette model. Numbers in [...] brackets denote the χ^2/d.o.f. For comparison relevant reference values for the 3D $O(3)$ universality class are given in the last line.

α_c	ν^a	β/ν^b	η^c
$1.9096-\sigma$	0.712(4) [1.8]	0.516(2) [0.5]	0.026(2) [0.2]
1.9096	0.711(4) [1.8]	0.518(2) [1.1]	0.029(5) [0.8]
$1.9096+\sigma$	0.710(4) [1.8]	0.519(3) [2.5]	0.032(7) [1.4]
1.9107[d]	0.709(3) [1.7]	0.525(8) [15.3]	0.051(10) [12]
$1.8230-\sigma$	0.708(4) [0.99]	0.515(2) [0.84]	0.025(4) [0.15]
1.8230	0.706(4) [1.04]	0.516(2) [0.40]	0.028(3) [0.31]
$1.8230+\sigma$	0.706(4) [1.10]	0.517(2) [1.6]	0.031(5) [0.80]
Ref. 49	0.7112(5)	0.518(1)	0.0375(5)

[a] $L > 12$.
[b] $L > 16$.
[c] $L > 20$.
[d] Previous best estimate of Ref. 19.

S. Wenzel and W. Janke, *Phys. Rev. B* **79**, 014410 (2009)
M. Troyer, M. Imada, and K. Ueda, *J. Phys. Soc. Japan* (1997)

Quantum Monte Carlo - critical exponents

Table IV: Fit results for the critical exponents ν, β/ν, and η. We summarize results including a variation of the critical point within its error bar. For the ladder model (top group of values) fit results and quality of fits are also given at the previous best estimate of α_c. The bottom group are results for the plaquette model. Numbers in [...] brackets denote the χ^2/d.o.f. For comparison relevant reference values for the 3D $O(3)$ universality class are given in the last line.

α_c	ν^a	β/ν^b	η^c
$1.9096-\sigma$	0.712(4) [1.8]	0.516(2) [0.5]	0.026(2) [0.2]
1.9096	0.711(4) [1.8]	0.518(2) [1.1]	0.029(5) [0.8]
$1.9096+\sigma$	0.710(4) [1.8]	0.519(3) [2.5]	0.032(7) [1.4]
1.9107^d	0.709(3) [1.7]	0.525(8) [15.3]	0.051(10) [12]
$1.8230-\sigma$	0.708(4) [0.99]	0.515(2) [0.84]	0.025(4) [0.15]
1.8230	0.706(4) [1.04]	0.516(2) [0.40]	0.028(3) [0.31]
$1.8230+\sigma$	0.706(4) [1.10]	0.517(2) [1.6]	0.031(5) [0.80]
Ref. 49	0.7112(5)	0.518(1)	0.0375(5)

$^a L > 12$.
$^b L > 16$.
$^c L > 20$.
^{d}Previous best estimate of Ref. 19.

Field-theoretic RG of CFT3
E. Vicari *et al.*

S. Wenzel and W. Janke, *Phys. Rev. B* **79**, 014410 (2009)
M. Troyer, M. Imada, and K. Ueda, *J. Phys. Soc. Japan* (1997)

$TlCuCl_3$

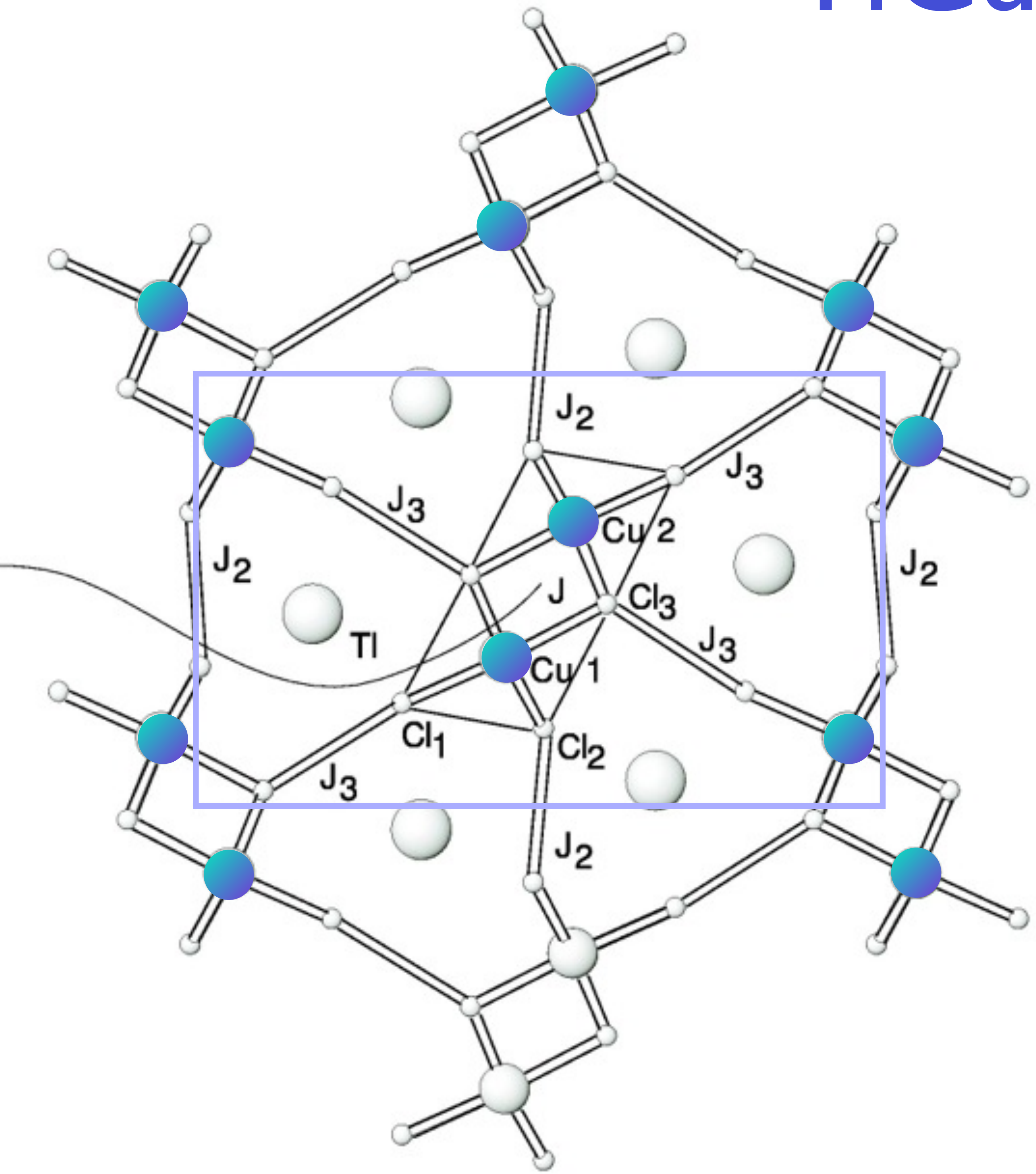

J2
J3
J2
Cu 2
J3
J2
J
Cl3
Tl
Cu 1
J3
Cl1
Cl2
J3
J2

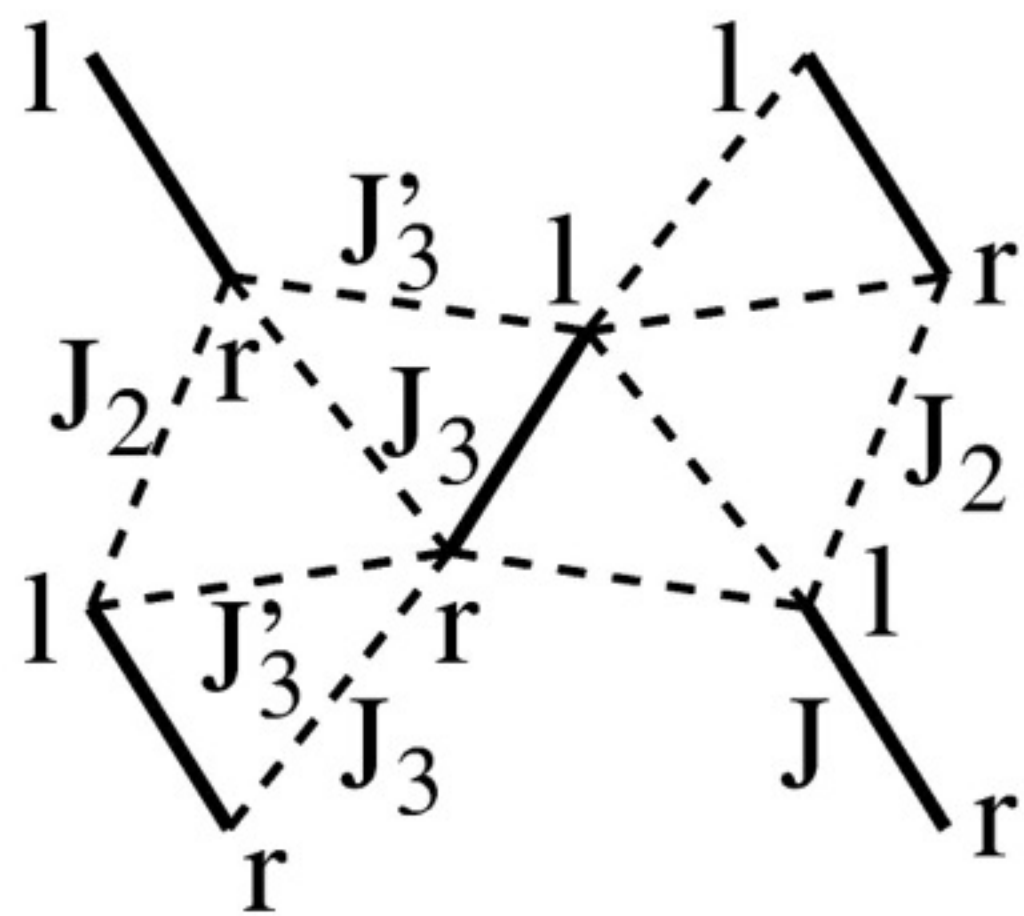

l
l
J'3
r
l
r
J2
J3
J2
l
r
l
J'3
J3
J
r
r

$TlCuCl_3$

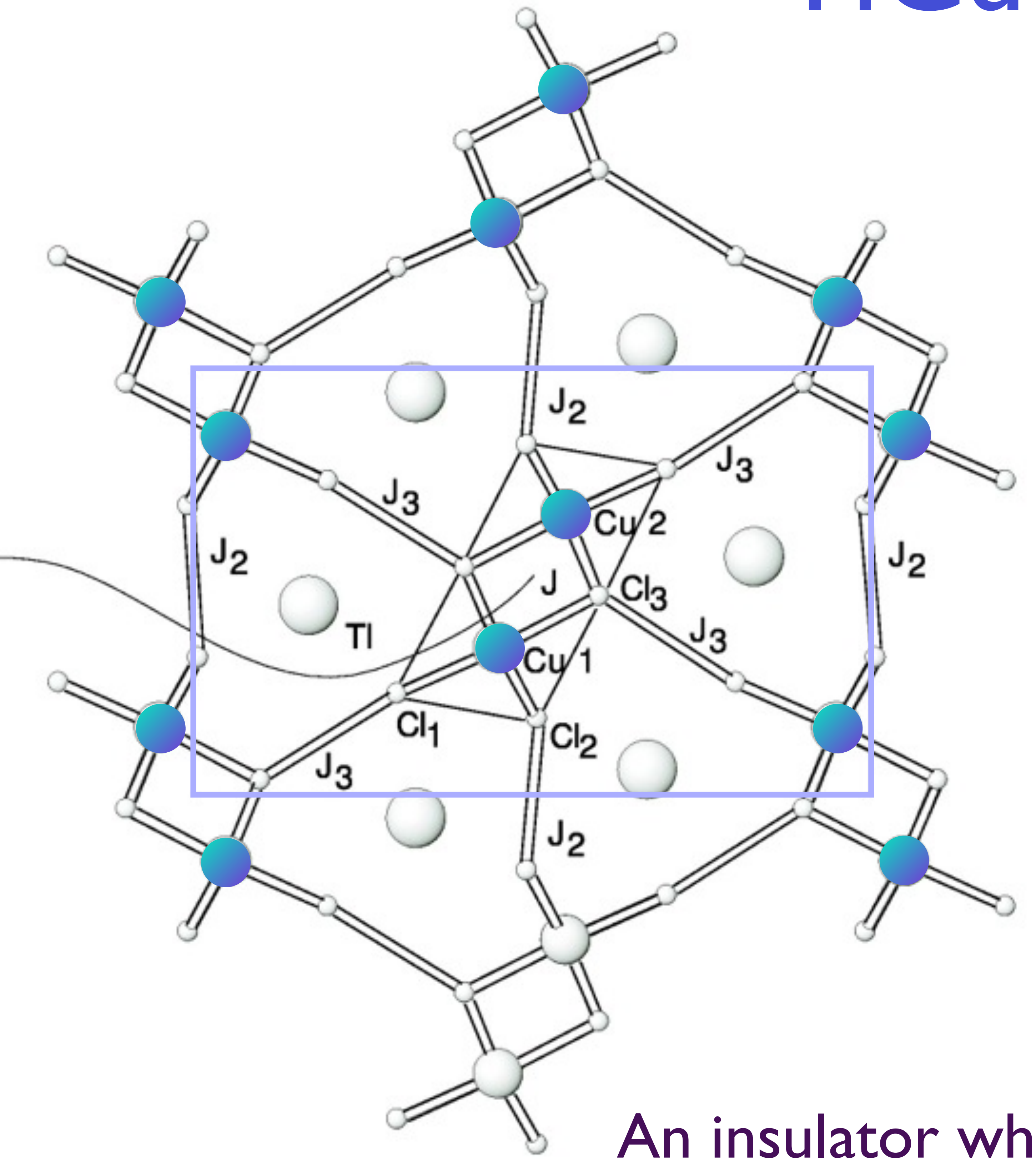

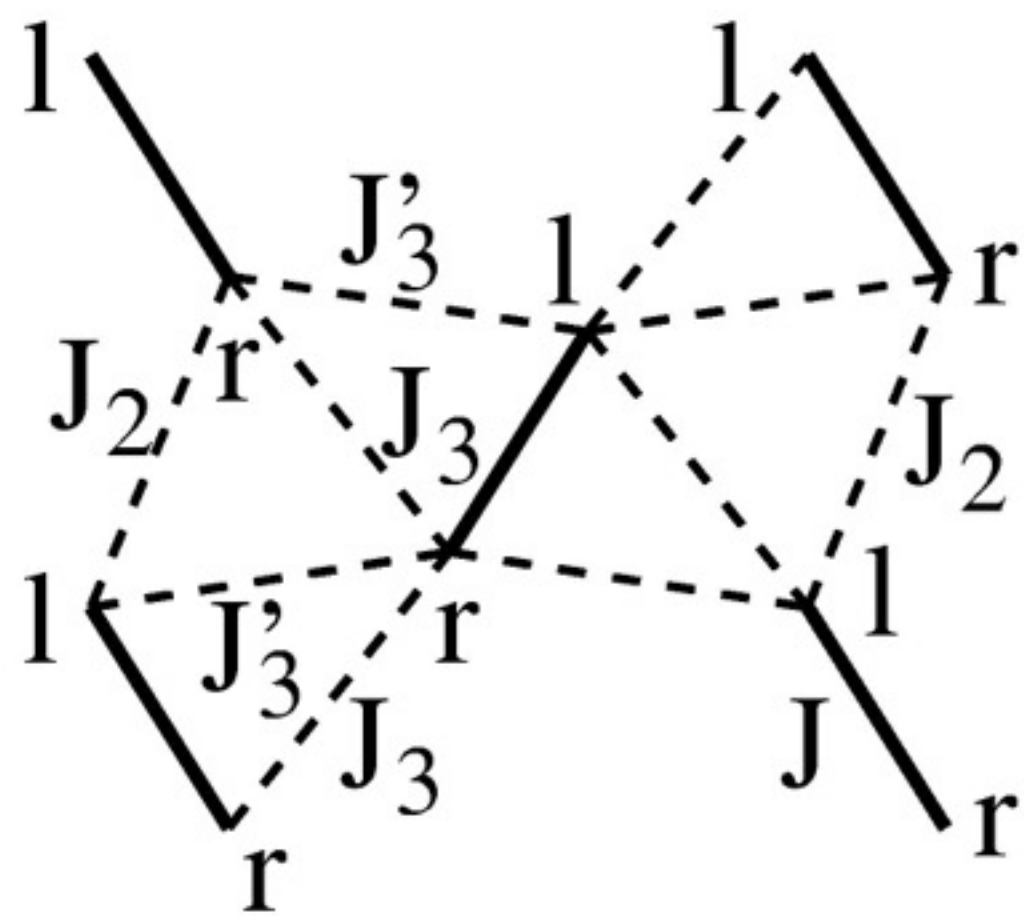

An insulator whose spin susceptibility vanishes exponentially as the temperature T tends to zero.

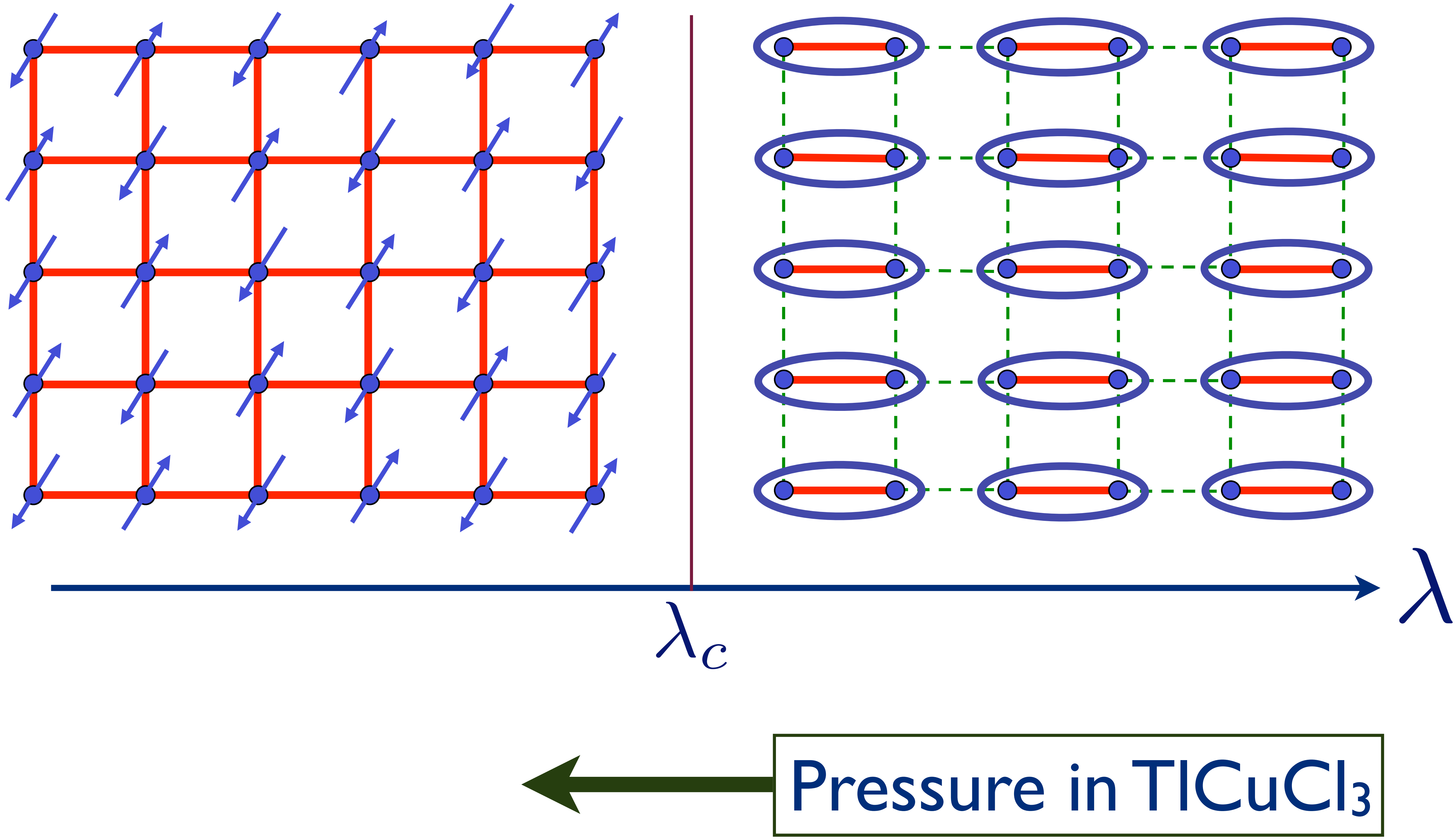

λ
λ_c
Pressure in $TlCuCl_3$

$TlCuCl_3$ at ambient pressure

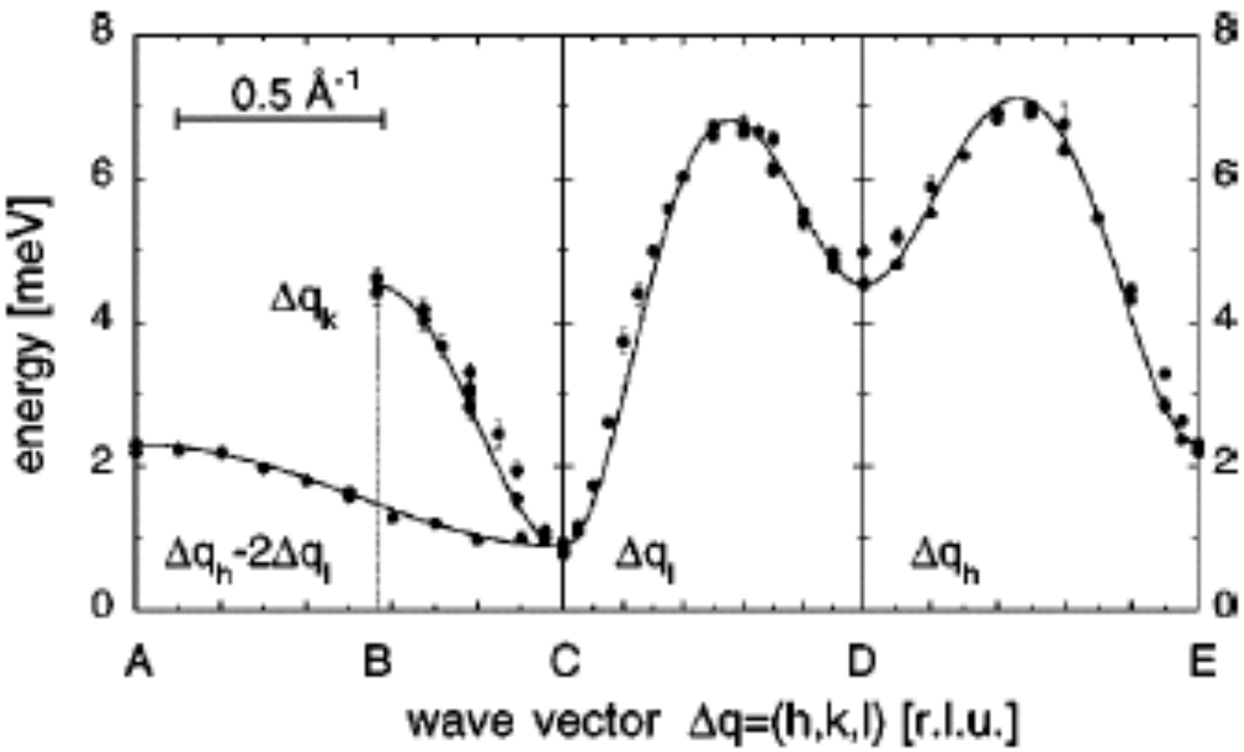

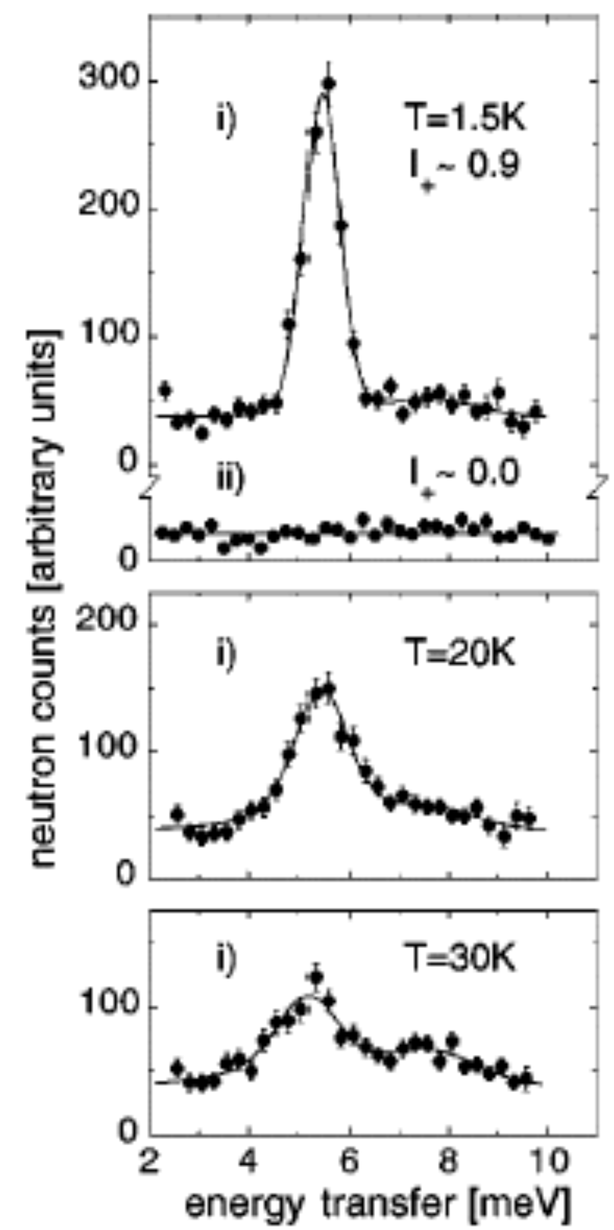

FIG. 1. Measured neutron profiles in the a^*c^* plane of $TlCuCl_3$ for $i=(1.35,0,0)$, $ii=(0,0,3.15)$ [r.l.u]. The spectrum at $T=1.5$ K

N. Cavadini, G. Heigold, W. Henggeler, A. Furrer, H.-U. Güdel, K. Krämer and H. Mutka, *Phys. Rev*. B 63 172414 (2001).

$TlCuCl_3$ at ambient pressure

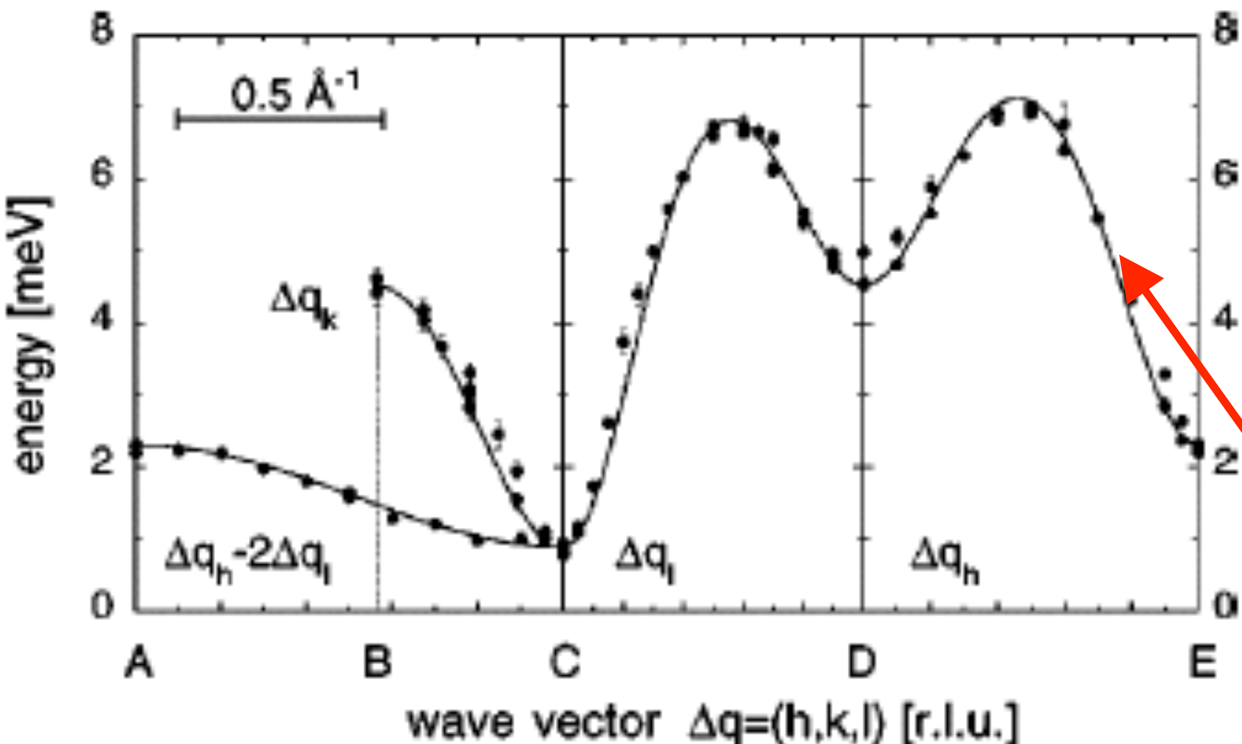

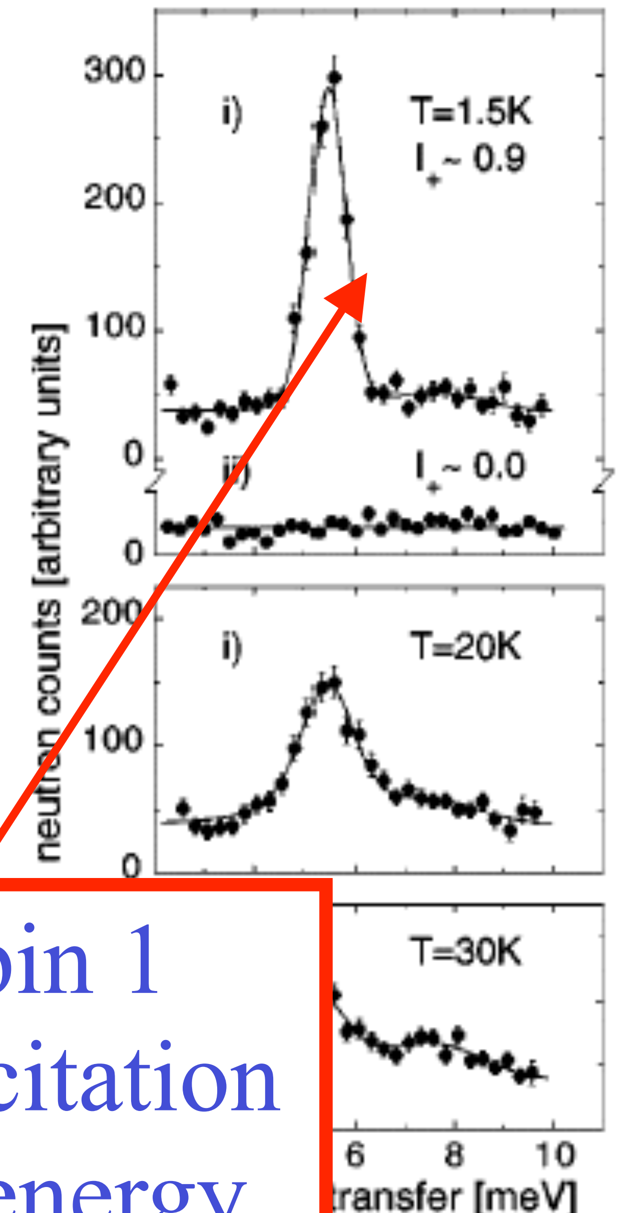

Sharp spin 1 particle excitation above an energy gap (spin gap)

…iles in the a^*c^* plane of $TlCuCl_3$ … [r.l.u]. The spectrum at $T = 1.5$ K

N. Cavadini, G. Heigold, W. Henggeler, A. Furrer, H.-U. Güdel, K. Krämer and H. Mutka, *Phys. Rev.* B 63 172414 (2001).

$TlCuCl_3$ with varying pressure

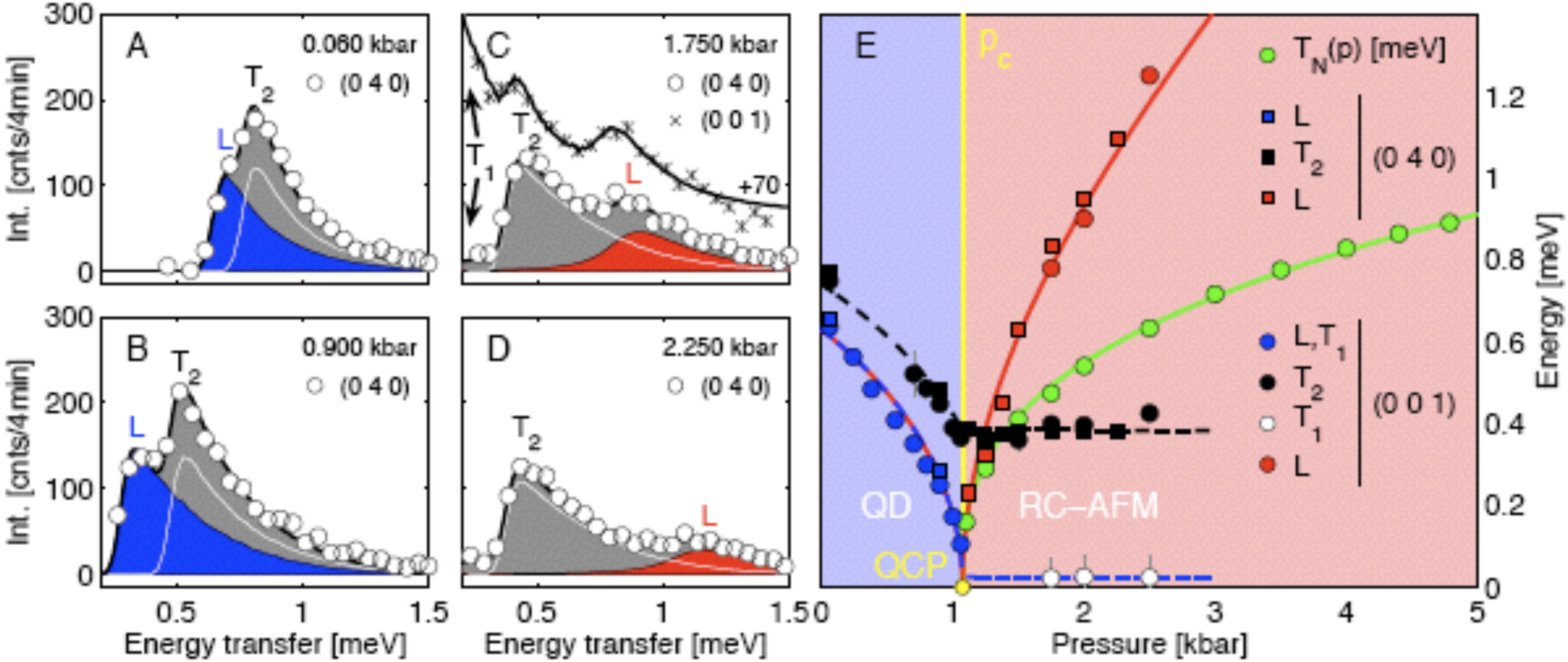

Observation of $3 \to 2$ low energy modes, emergence of new longitudinal mode (the "Higgs boson") in Néel phase, and vanishing of Néel temperature at quantum critical point

Christian Ruegg, Bruce Normand, Masashige Matsumoto, Albert Furrer, Desmond McMorrow, Karl Kramer, Hans–Ulrich Gudel, Severian Gvasaliya, Hannu Mutka, and Martin Boehm, *Phys. Rev. Lett.* **100**, 205701 (2008)

Prediction of quantum field theory

Potential for $\vec{\varphi}$ fluctuations: $V(\vec{\varphi}) = (\lambda - \lambda_c)\vec{\varphi}^2 + u\left(\vec{\varphi}^2\right)^2$

Paramagnetic phase, $\lambda > \lambda_c$

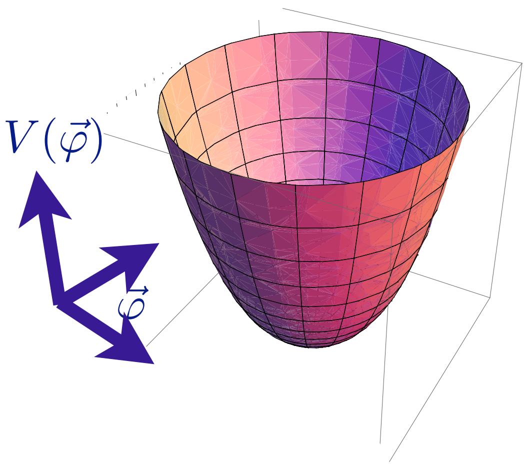

Expand about $\vec{\varphi} = 0$:

$$V(\vec{\varphi}) \approx (\lambda - \lambda_c)\vec{\varphi}^2$$

Yields 3 particles with energy gap $\sim \sqrt{(\lambda - \lambda_c)}$

Prediction of quantum field theory

Potential for $\vec{\varphi}$ fluctuations: $V(\vec{\varphi}) = (\lambda - \lambda_c)\vec{\varphi}^2 + u\left(\vec{\varphi}^2\right)^2$

Paramagnetic phase, $\lambda > \lambda_c$

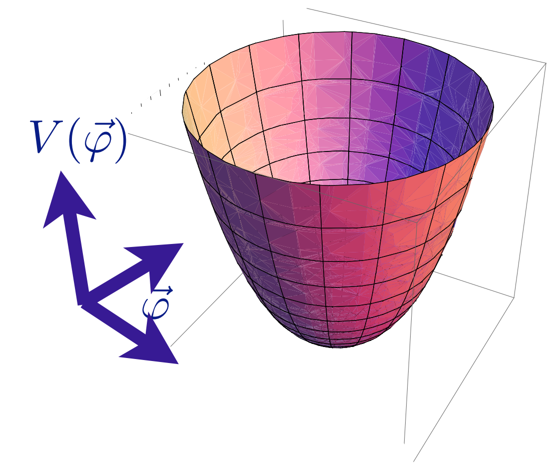

Expand about $\vec{\varphi} = 0$:

$$V(\vec{\varphi}) \approx (\lambda - \lambda_c)\vec{\varphi}^2$$

Yields 3 particles with energy gap $\sim \sqrt{(\lambda - \lambda_c)}$

Néel phase, $\lambda < \lambda_c$

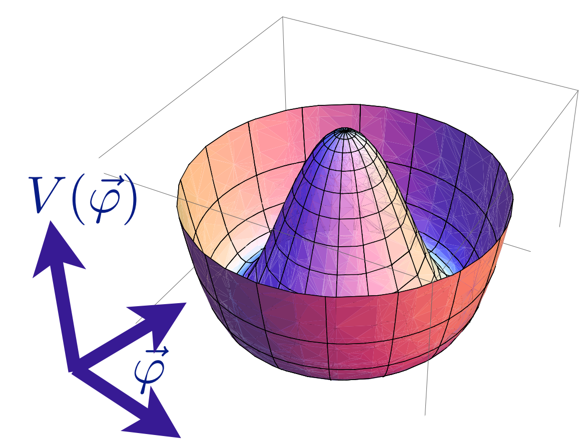

Expand $\vec{\varphi} = \left(0, 0, \sqrt{(\lambda_c - \lambda)/(2u)}\right) + \vec{\varphi}_1$:

$$V(\vec{\varphi}) \approx 2(\lambda_c - \lambda)\varphi_{1z}^2$$

Yields 2 gapless spin waves and one Higgs particle with energy gap $\sim \sqrt{2(\lambda_c - \lambda)}$

Prediction of quantum field theory

$$\frac{\text{Energy of Higgs particle}}{\text{Energy of triplon}} = \sqrt{2}$$

$$V(\vec{\varphi}) = (\lambda - \lambda_c)\vec{\varphi}^2 + u\left(\vec{\varphi}^2\right)^2$$

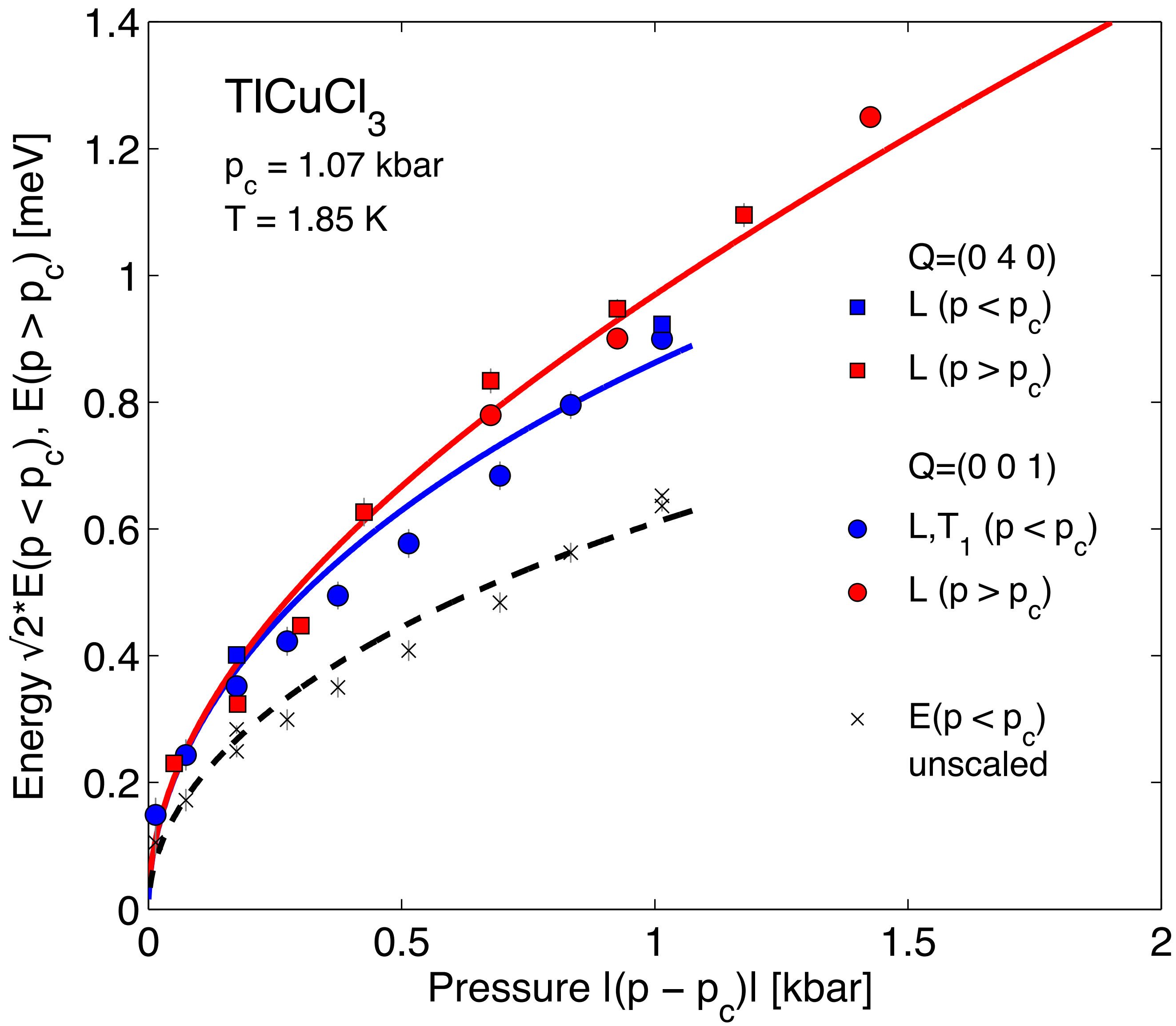

S. Sachdev, arXiv:0901.4103

Quantum criticality at non-zero temperature